AMERICAN SOCIETY FOR MICROBIOLOGY | Applied and Environmental Microbiology®

PHYSIOLOGY

Hybrid Two-Component Sensors for Identification of Bacterial Chemoreceptor Function

Rita A. Luu,[a]* Rebecca A. Schomer,[a] Ceanne N. Brunton,[a]* Richard Truong,[a]* Albert P. Ta,[a]* Watumesa A. Tan,[a]* Juanito V. Parales,[a] Yu-Jing Wang,[c] Yu-Wen Huo,[c] Shuang-Jiang Liu,[c] Jayna L. Ditty,[b] Valley Stewart,[a] Rebecca E. Parales[a]

[a]Department of Microbiology and Molecular Genetics, College of Biological Sciences, University of California, Davis, Davis, California, USA
[b]Department of Biology, College of Arts and Sciences, University of St. Thomas, St. Paul, Minnesota, USA
[c]State Key Laboratory of Microbial Resources, Institute of Microbiology, Chinese Academy of Sciences, Beijing, China

ABSTRACT Soil bacteria adapt to diverse and rapidly changing environmental conditions by sensing and responding to environmental cues using a variety of sensory systems. Two-component systems are a widespread type of signal transduction system present in all three domains of life and typically are comprised of a sensor kinase and a response regulator. Many two-component systems function by regulating gene expression in response to environmental stimuli. The bacterial chemotaxis system is a modified two-component system with additional protein components and a response that, rather than regulating gene expression, involves behavioral adaptation and results in net movement toward or away from a chemical stimulus. Soil bacteria generally have 20 to 40 or more chemoreceptors encoded in their genomes. To simplify the identification of chemoeffectors (ligands) sensed by bacterial chemoreceptors, we constructed hybrid sensor proteins by fusing the sensor domains of *Pseudomonas putida* chemoreceptors to the signaling domains of the *Escherichia coli* NarX/NarQ nitrate sensors. Responses to potential attractants were monitored by β-galactosidase assays using an *E. coli* reporter strain in which the nitrate-responsive *narG* promoter was fused to *lacZ*. Hybrid receptors constructed from PcaY, McfR, and NahY, which are chemoreceptors for aromatic acids, tricarboxylic acid cycle intermediates, and naphthalene, respectively, were sensitive and specific for detecting known attractants, and the β-galactosidase activities measured in *E. coli* correlated well with results of chemotaxis assays in the native *P. putida* strain. In addition, a screen of the hybrid receptors successfully identified new ligands for chemoreceptor proteins and resulted in the identification of six receptors that detect propionate.

IMPORTANCE Relatively few of the thousands of chemoreceptors encoded in bacterial genomes have been functionally characterized. More importantly, although methyl-accepting chemotaxis proteins, the major type of chemoreceptors present in bacteria, are easily identified bioinformatically, it is not currently possible to predict what chemicals will bind to a particular chemoreceptor. Chemotaxis is known to play roles in biodegradation as well as in host-pathogen and host-symbiont interactions, but many studies are currently limited by the inability to identify relevant chemoreceptor ligands. The use of hybrid receptors and this simple *E. coli* reporter system allowed rapid and sensitive screening for potential chemoeffectors. The fusion site chosen for this study resulted in a high percentage of functional hybrids, indicating that it could be used to broadly test chemoreceptor responses from phylogenetically diverse samples. Considering the wide range of chemical attractants detected by soil bacteria, hybrid receptors may also be useful as sensitive biosensors.

KEYWORDS *Pseudomonas putida*, biosensor, methyl-accepting chemotaxis protein, receptor, two-component system

Citation Luu RA, Schomer RA, Brunton CN, Truong R, Ta AP, Tan WA, Parales JV, Wang Y-J, Huo Y-W, Liu S-J, Ditty JL, Stewart V, Parales RE. 2019. Hybrid two-component sensors for identification of bacterial chemoreceptor function. Appl Environ Microbiol 85:e01626-19. https://doi.org/10.1128/AEM.01626-19.

Editor Gladys Alexandre, University of Tennessee at Knoxville

Address correspondence to Rebecca E. Parales, reparales@ucdavis.edu.

* Present address: Rita A. Luu, List Biological Laboratories, Inc., Campbell, California, USA; Ceanne N. Brunton, Novozymes, Davis, California, USA; Richard Truong, BioMarin Pharmaceutical, Inc., Novato, California, USA; Albert P. Ta, Department of Physiology and Biophysics, University of California, Irvine, School of Medicine, Irvine, California, USA; Watumesa A. Tan, Faculty of Biotechnology, Atma Jaya Catholic University of Indonesia, Jakarta, Indonesia.

Received 19 July 2019
Accepted 31 August 2019
Accepted manuscript posted online 6 September 2019
Published 30 October 2019

Signal transduction pathways play an essential role in the survival and adaptation of bacteria in response to environmental changes. Two-component regulatory systems, which in their simplest form are composed of a sensor protein and a response regulator, are integral in sensing environmental stimuli and relaying the information to the cell (reviewed in reference 1). Two well-characterized two-component systems in *Escherichia coli* are the nitrate-responsive sensory proteins NarX/NarQ and their corresponding response regulators NarL/NarP (reviewed in reference 2). Under anoxic conditions, nitrate respiration is energetically more favorable than other anaerobic respiratory or fermentative pathways, and the NarX/L and NarQ/P two-component systems are used by *E. coli* to detect the presence of nitrate and turn on the genes for nitrate respiration. NarX and NarQ are transmembrane sensory histidine kinases that autophosphorylate when bound to nitrate and nitrite and then donate phosphoryl groups to NarL and NarP. The phosphorylated forms of NarL and NarP are transcriptional activators that bind to nitrate-responsive promoters to activate the transcription of genes encoding the nitrate respiration enzymes, such as nitrate reductase. NarX/NarQ hybrid sensors have been constructed to elucidate the structural elements important for sensing and signaling in two-component systems (3, 4). Many of these studies involved the use of a strain in which the NarL-responsive *narG* promoter was fused to a *lacZ* reporter gene (5) so that NarX/NarQ kinase activity resulting from nitrate binding can be easily measured as increased β-galactosidase activity.

Methyl-accepting chemotaxis proteins (MCPs) represent another important group of signal transduction proteins that share sensory domain architecture similar to that found in two-component systems (6, 7). MCPs are transmembrane chemoreceptors that detect chemical attractants and repellents and transmit the chemotaxis signal to the flagellar motor(s) via a phosphorylation cascade (reviewed in references 8 and 9). However, MCPs do not have a histidine kinase function like other two-component sensory proteins but rather rely on the adaptor protein CheW to link the MCP to a histidine kinase called CheA. In the absence of an attractant or in response to increasing repellent concentrations, CheA autophosphorylates a conserved histidine residue, and the phosphoryl group is donated to the response regulator CheY. Phosphorylated CheY binds to the flagellar motor, causing a switch in the direction of flagellar rotation and a random change in swimming direction. In contrast, increasing concentrations of an attractant inhibit CheA autophosphorylation, and as a consequence, CheY remains unphosphorylated, which reduces the rate of motor switching and results in longer periods of smooth swimming up the gradient of the attractant. MCPs share a signaling motif called HAMP (histidine kinase, adenylyl cyclase, MCP, and phosphatase) with other membrane-associated sensory systems, such as NarX/Q (reviewed in reference 10). The HAMP domain connects the periplasmic ligand-binding domain (LBD) of the MCP to the cytoplasmic signaling domain and is essential for transmitting the sensory signal.

Bacteria are faced with constant environmental changes in pH, nutrients, and oxygen, and chemotaxis allows them to sense these changes and move toward niches that are optimal for their survival and growth. The number of MCPs varies between microbial species and often reflects their metabolic diversity and lifestyle (11). For example, *Escherichia coli*, which has four MCPs and one MCP-like energy taxis receptor, mainly senses nutrients such as simple sugars and amino acids and also signaling molecules like AI-2 and indole (12–14). In contrast, the more metabolically versatile *Pseudomonas putida* strains have at least 25 MCPs or MCP-like proteins. In addition to sugars and amino acids, *P. putida* is known to sense a wide range of naturally occurring and xenobiotic aromatic compounds (14, 15).

To date, relatively few MCPs and MCP-like proteins from soil bacteria have been characterized, but ligands for several MCPs from various pseudomonads and rhizobia have been characterized in recent years (14, 16). Although there are numerous known attractants and repellents for various soil bacteria, the relevant chemoreceptors often remain unidentified due to various technical constraints in current methods (16). Previous studies have utilized the construction of hybrid receptors to help elucidate the

protein function of *E. coli* MCPs (17, 18), *E. coli* Nar proteins (3), and Nar-MCP chimeras (19, 20). In this study, we constructed MCP-Nar hybrid receptors and expressed them in an *E. coli* reporter strain (i) to test if their readout is an accurate proxy for chemotactic responses, (ii) to test whether hybrid receptors have the potential to be used as sensitive biosensors, and (iii) to develop a rapid and quantitative method to identify the ligands of MCPs of unknown function.

RESULTS

***In vitro* binding of the PcaY LBD to selected attractants.** As a proof of concept to validate the function, sensitivity, and specificity of MCP-Nar hybrid receptors, we first generated hybrids of the aromatic acid receptor PcaY from *P. putida* F1. This MCP detects a wide range of aromatic acids and hydroaromatic compounds as attractants and mediates weak to very strong responses depending on the attractant (21). Two lines of evidence suggested that these attractants bind directly to the receptor: the finding that a catabolic mutant unable to catabolize vanillate still responded to vanillate and the observation that the response to nonmetabolizable substituted benzoates was mediated by PcaY (21). These findings, however, did not rule out the possibility that a periplasmic binding protein could serve as the primary chemoreceptor. Here, binding of the PcaY LBD to ligands was verified *in vitro* by isothermal titration calorimetry (ITC). As shown in Fig. 1, the PcaY LBD bound to 4-hydroxybenzoate (4-HBA), quinate, vanillate, and shikimate with K_d (dissociation constant) values of 5.5, 7.7, 10, and 37 μM, respectively (Table 1). The ΔH values for 4-HBA, quinate, vanillate, and shikimate were calculated to be −161, −177, −67.4, and −177 kJ/mol, respectively. Binding was driven by very favorable enthalpy changes (ΔH) and counterbalanced by large unfavorable entropy changes ($T\Delta S$), which were −131, −148, −59.6, and −149 kJ/mol for 4-HBA, quinate, vanillate, and shikimate, respectively. As a consequence, for all of these reactions, the Gibbs free energy ($\Delta G = \Delta H - T\Delta S$) values were negative. Benzoate, a good growth substrate and attractant, and 4-nitrobenzoate (4-NBA), a nonmetabolizable aromatic acid that serves as a weak attractant for *P. putida* F1 (21), were found to bind to the PcaY LBD (Fig. 1) but with higher K_d values (96 μM and 60 μM, respectively). In contrast, 2-chlorobenzoate (2-CBA), which elicited a barely detectable chemotactic response in *P. putida* F1 (21), did not bind to the PcaY LBD at the concentrations tested (see Fig. S1 in the supplemental material). Although vanillin is a weak attractant for *P. putida* F1 (21), based on ITC, there was no binding between vanillin and the PcaY LBD, even when the concentration of PcaY was increased from 100 to 258 μM or the concentration of vanillin was increased from 0.5 to 1 mM (Fig. S1). Control experiments with citrate, which is known to be detected by a different MCP in *P. putida* F1 (McfQ) (22), showed no binding to the PcaY LBD (Fig. S1). In addition, according to the ITC results, there was no binding between the PcaY LBD and *p*-coumarate (1 mM) (Fig. S1), a structurally related aromatic acid that we recently showed is sensed via the energy taxis receptor Aer-2 in *P. putida* F1 (23). These results provide direct evidence that the PcaY LBD binds specifically to chemicals that are sensed by PcaY in *P. putida* F1 and are consistent with ITC results with the PcaY LBD from *P. putida* KT2440 (Table 1) (24).

Construction of MCP-Nar hybrid sensors. To construct hybrid PcaY-Nar receptors, we first aligned amino acid sequences of the HAMP domains of PcaY with those of the Nar proteins NarQ and NarX (Fig. 2A) along with those of the *E. coli* MCP Tsr and the *Salmonella enterica* MCP Tar for comparison. Based on these sequence alignments and junction points of previously constructed functional hybrids of NarX and NarQ (3), four PcaY-Nar hybrid receptors were generated with different junction points as described in Materials and Methods and as shown in Fig. 2A and B. Two hybrids containing the HAMP domains of the NarX and NarQ proteins, respectively, were generated. In one, Pro217 of the LBD of PcaY was joined to NarX at Trp182 (designated PcaY-NarXHAMP) or NarQ at Leu180 (PcaY-NarQHAMP), a junction point that had previously resulted in functional hybrids between NarX and CpxA and between NarQ and NarX (3). Two additional hybrids containing the HAMP domain of PcaY were constructed: in one,

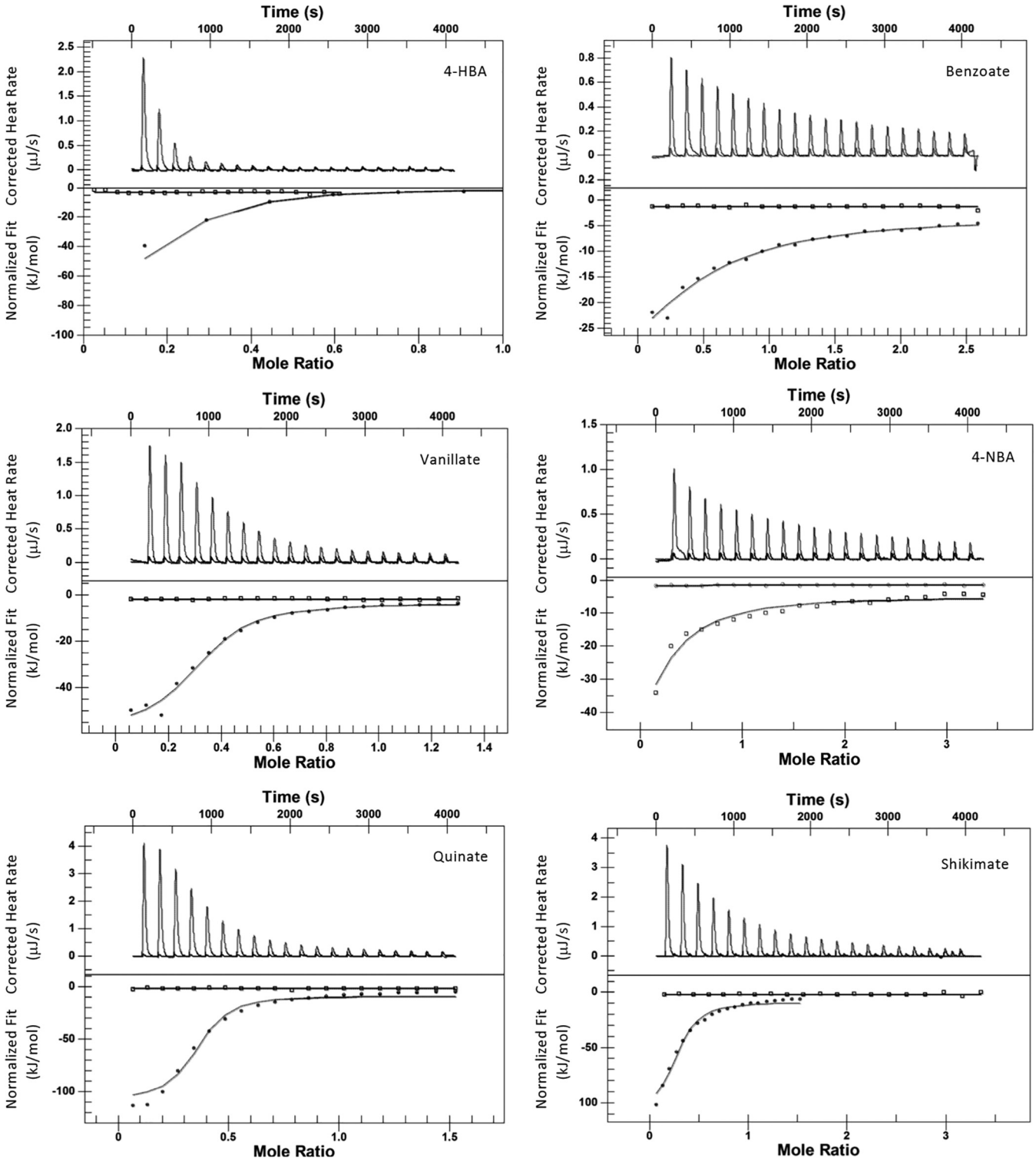

FIG 1 Results of ITC experiments to measure binding of ligands to the PcaY LBD. Binding of the aromatic compounds 4-hydroxybenzoate (4-HBA), benzoate, 4-nitrobenzoate (4-NBA), and vanillate and the hydroaromatic compounds quinate and shikimate, which are sensed by *P. putida* F1 via PcaY, was tested.

Ser258 of PcaY was joined to NarQ at Leu222 (PcaYHAMP-NarQ) (Fig. 2), as in the previously reported NarX-NarQ-5 hybrid (3). According to sequence alignments, leucine 222, which is located at the end of the AS2 region of the HAMP domain, is conserved in NarX, NarQ, and the MCPs Tar and Tsr (Fig. 2A), whereas in the PcaY HAMP domain,

TABLE 1 PcaY binding constants determined by ITC and estimated from β-galactosidase activities[c]

Ligand	K_d of PcaY LBD (μM)	K_d of PcaY_PP LBD[a] (μM)	Estimated binding affinity[b] (μM)
4-HBA	5.5	7.2	15
Benzoate	96	90	316
Protocatechuate	ND	6.4	15
Vanillate	10	10	112
Quinate	7.7	3.7	10
Shikimate	37	37	66
4-Nitrobenzoate	60	61	ND

[a]Data for PcaY from *P. putida* KT2440 (24).
[b]Estimated from a plot of the relative β-galactosidase activity versus the ligand concentration using Prism (see Materials and Methods and Fig. S3).
[c]ND, not determined.

a glutamine residue is present at the corresponding position. Therefore, to determine whether this specific amino acid is important for signaling, a construct with an L222Q substitution was also made (PcaYHAMP-NarQ^{L222Q}).

The PcaY-NarQHAMP hybrid sensor is functional in *E. coli*. To test whether the hybrid receptors are functional, each of the constructs was introduced into the *E. coli* reporter strain VJS5054, in which the nitrate-responsive *narG* promoter is fused to *lacZ* [Φ(*narG-lacZ*)], which allows rapid detection of NarX and NarQ signaling using β-galactosidase assays (5) (Fig. S2). *E. coli* VJS5054 carrying each construct was grown anaerobically in the presence and absence of 4-HBA, a known attractant for PcaY, and the expression of *lacZ* was monitored using β-galactosidase assays. In bacterial che-

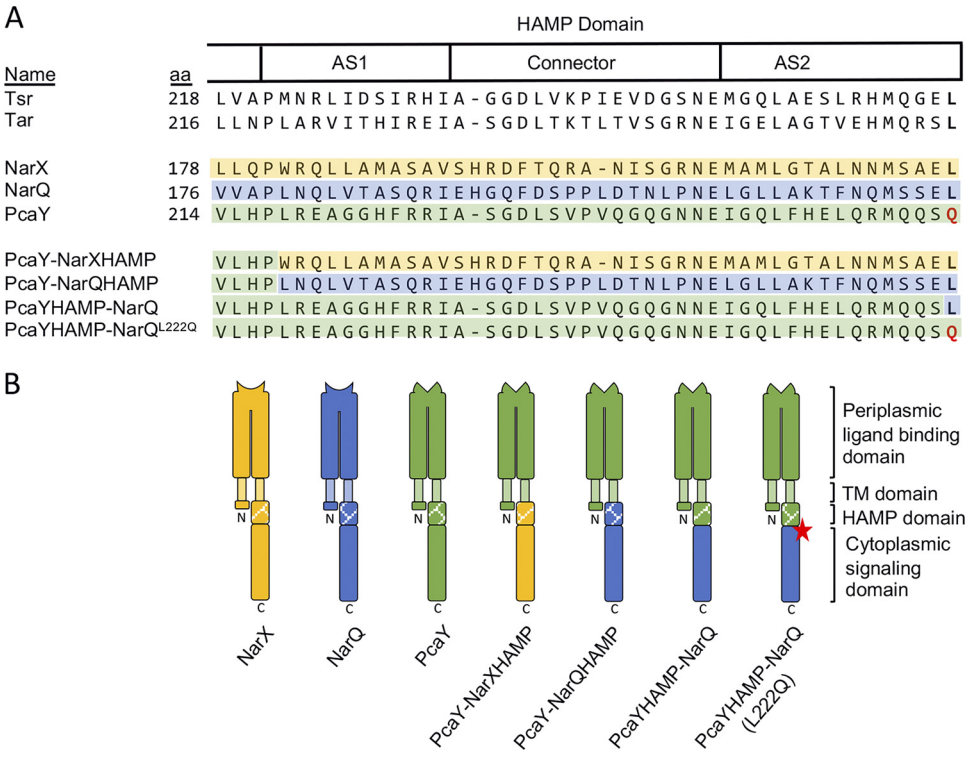

FIG 2 Design of PcaY-Nar hybrids. (A) Amino acid (aa) sequence alignments of the HAMP domains in Tar (from *Salmonella enterica*); Tsr, NarX, and NarQ (from *E. coli*); PcaY (from *P. putida* F1); and the constructed PcaY-NarX/Q hybrids. The HAMP domain consists of two amphipathic helices (AS1 and AS2) joined by an unstructured connecting sequence (3, 70). Sequences from NarX, NarQ, and PcaY are highlighted in blue, yellow, and green, respectively. (B) Schematic diagram displaying the elements of NarX, NarQ, and PcaY in the hybrid constructs. Segments from NarX, NarQ, and PcaY are shown in yellow, blue, and green, respectively. The red star denotes the approximate location of the L222Q amino acid substitution in PcaYHAMP-NarQ^{L222Q}.

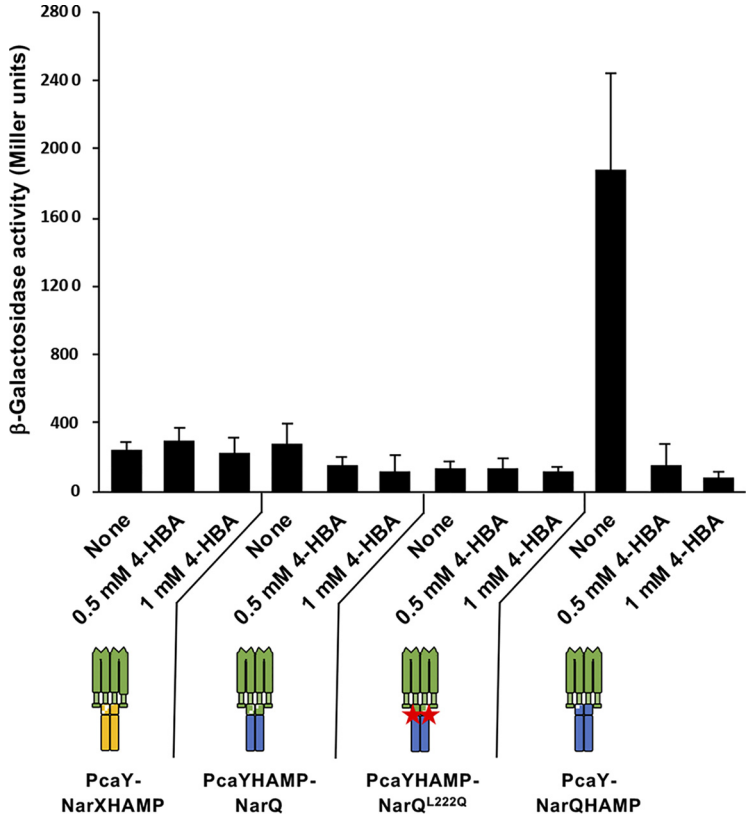

FIG 3 Φ(*narG-lacZ*) expression in *E. coli* VJS5054 carrying the four PcaY-Nar hybrid constructs. Responses to 0.5 mM and 1 mM 4-HBA were tested. A schematic model of the four hybrids is shown, with elements from NarX, NarQ, and PcaY denoted in yellow, blue, and green, respectively. β-Galactosidase activity is reported in Miller units, and results are the averages from at least three independent experiments, with error bars representing standard deviations.

motaxis, the MCP is in the "off" state when the ligand is bound (Fig. S2). In this state, the level of phosphorylation of the response regulator CheY is low, resulting in fewer changes in the direction of flagellar rotation (i.e., fewer tumbles) and, consequently, longer periods of smooth swimming toward the attractant (8). In contrast, nitrate binding of NarQ or NarX produces an "on" state, resulting in greater phosphorylation of the response regulator NarL and transcriptional activation of the nitrate-responsive promoter (2). Since the PcaY sensing domain in the hybrid sensors is fused to the NarX/Q signaling domain, binding of the attractant to the LBD of the hybrid receptor would result in less phosphorylation of the response regulator NarL, which in turn would reduce expression from the *narG* promoter (Fig. S2) and result in lower β-galactosidase activity. Therefore, the default state of functional hybrid receptors would be "on," resulting in high levels of β-galactosidase activity; when the cognate attractant is added, the receptor would shift to the "off" state, resulting in lower β-galactosidase activity.

E. coli VJS5054 cultures carrying the various PcaY-NarX/Q hybrid constructs were tested for responses to 0.5 mM and 1 mM 4-HBA (Fig. 3). Of the four hybrids, only PcaY-NarQHAMP showed high Φ(*narG-lacZ*) expression levels in the absence of a ligand and a significant decrease in Φ(*narG-lacZ*) expression in response to 0.5 mM and 1 mM 4-HBA (~15- and 27-fold reductions, respectively). Although VJS5054 carrying PcaYHAMP-NarQ had low Φ(*narG-lacZ*) expression levels, it showed a weak concentration-independent response (~2-fold reduction in β-galactosidase activity in response to either 0.5 mM or 1 mM 4-HBA). In contrast, strains carrying PcaY-NarXHAMP and PcaYHAMP-NarQ^{L222Q} had low β-galactosidase activity and showed no response to the presence of the attractant (Fig. 3). Therefore, PcaY-NarQHAMP (the hybrid in which

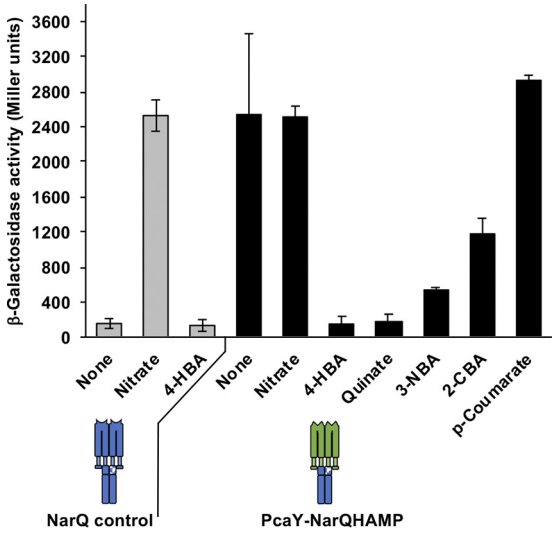

FIG 4 Φ(*narG-lacZ*) expression in *E. coli* VJS5054 carrying the native NarQ and PcaY-NarQ hybrid receptors. β-Galactosidase activity in response to the presence of 40 mM nitrate or 1 mM 4-HBA, quinate, 3-nitrobenzoate (3-NBA), 2-chlorobenzoate (2-CBA), or *p*-coumarate was monitored. β-Galactosidase activity is reported in Miller units, and the results are the averages from at least three independent experiments, with error bars representing standard deviations.

PcaY is fused to NarQ via the native NarQ HAMP domain) was selected for further characterization. For simplicity, we refer to this functional construct as PcaY-NarQ.

The hybrid PcaY-NarQ sensor responds only to compounds that are sensed as chemoattractants by PcaY in *P. putida* F1. To demonstrate that the responses seen with the PcaY-NarQ hybrid receptor were specific to the LBD of PcaY and not to an artifact of NarQ signaling, the wild-type NarQ construct was tested for responses to nitrate and 4-HBA. As expected, given the sensing mechanism of wild-type NarQ, the Φ(*narG-lacZ*) expression level was low in the absence of the ligand, and it increased ~15-fold in the presence of 40 mM nitrate (Fig. 4). β-Galactosidase activity remained low in the presence of 1 mM 4-HBA, indicating that NarQ itself cannot detect the aromatic attractant 4-HBA. Additionally, we tested the response of the strain carrying PcaY-NarQ to nitrate and failed to see a response (Fig. 4). Together, these results demonstrate that the changes in Φ(*narG-lacZ*) expression are due solely to binding of the ligand to the PcaY LBD.

Next, we tested a range of aromatic and hydroaromatic compounds to evaluate whether PcaY-NarQ can differentiate between chemicals that are known attractants sensed by PcaY in the native host and structurally similar compounds that are not sensed via PcaY. As shown in previous studies (21), quinate, 3-nitrobenzoate, and 2-chlorobenzoate are considered strong, moderate, and weak attractants sensed by PcaY, respectively, and although *p*-coumarate is an attractant for *P. putida* F1, the response is mediated by the energy taxis receptor Aer-2 but not PcaY (23). VJS5054 cells expressing PcaY-NarQ were grown in the absence (control) and presence of equimolar amounts (1 mM) of each of these compounds as well as 4-HBA, and expression of the Φ(*narG-lacZ*) operon fusion was monitored. As shown in Fig. 4, 4-HBA and quinate elicited the strongest responses (>10-fold decrease in activity), followed by 3-nitrobenzoate (5-fold decrease), and the weakest response was from 2-chlorobenzoate (2-fold decrease). These results correlate with the strength of the chemotactic responses to these compounds by *P. putida* F1 (21). Importantly, there was no response to *p*-coumarate even though this compound is similar in structure to the attractants sensed by PcaY (Fig. 4). These results demonstrate that the hybrid receptor specifically binds chemicals that are sensed as attractants via PcaY.

The chimeric receptor is sensitive to changes in attractant concentrations. We next examined the sensitivity of the hybrid receptor by varying the concentrations of

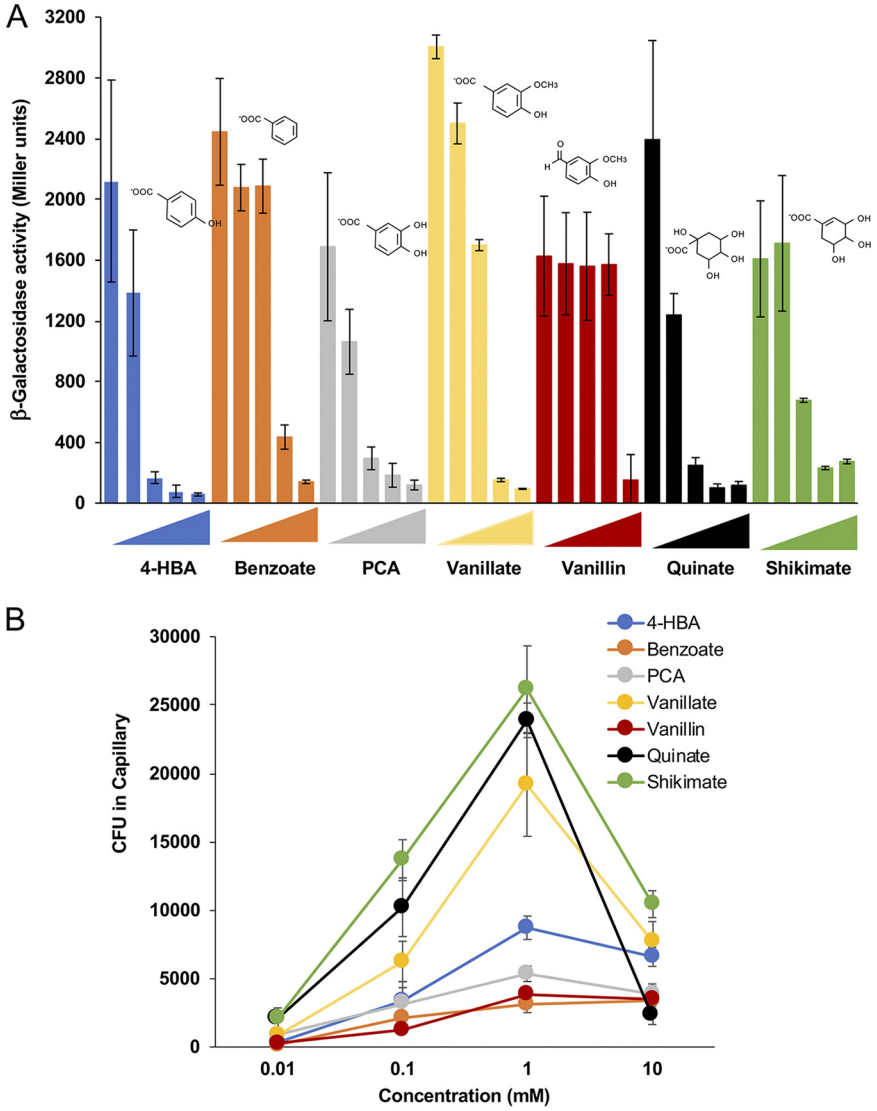

FIG 5 Comparison of the sensitivity of the hybrid PcaY-NarQ receptor in *E. coli* VJS5054 with that of the native chemoreceptor PcaY in *P. putida* F1. (A) Responses of the *E. coli* reporter strain carrying PcaY-NarQ to 4-HBA, benzoate, PCA, vanillate, vanillin, quinate, and shikimate measured using β-galactosidase assays. Colored triangles below the results indicate increasing concentrations of the ligand (0, 0.01, 0.1, 1.0, and 10 mM, respectively). Results are averages from at least three independent experiments, with error bars representing standard deviations. (B) Responses of wild-type *P. putida* F1 to 4-HBA, benzoate, PCA, vanillate, vanillin, quinate, and shikimate measured using quantitative capillary assays. The average number of cells in capillaries containing buffer only (170 $\pm$ 54 CFU/ml) was subtracted from each data set. Results shown are the averages from at least three independent experiments, and error bars represent the standard errors of the means. Results shown for quinate and 4-HBA were reported previously (21).

attractants sensed by PcaY to determine whether the response was concentration dependent. The *E. coli* reporter strain carrying the hybrid receptor PcaY-NarQ was grown anaerobically in the presence of 0.01, 0.1, 1.0, and 10 mM 4-HBA, benzoate, protocatechuate (PCA), vanillate, vanillin, quinate, or shikimate, and Φ(*narG-lacZ*) expression was monitored. The responses to all compounds were concentration dependent (Fig. 5A). Binding affinities were estimated from plots of the ligand concentration versus the ratio of LacZ activity in response to each chemical relative to that in the absence of an added ligand (Fig. S3); these values were remarkably similar to those determined *in vitro* by ITC (Table 1), especially since the estimations were made using only three or four ligand concentrations. In general, these results are also comparable

TABLE 2 Activity of hybrid *P. putida* F1 receptors

Hybrid receptor[a]	*P. putida* KT2440 MCP ortholog[a]	LBD type[b]	Avg β-galactosidase activity (− ligand) ± SD[c]	Avg β-galactosidase activity (+ ligand) ± SD[c]	Ligand tested (reference[s])[d]
NarQ wild-type control	NA	4HB	170 ± 5	2,660 ± 250	40 mM nitrate
PcaY-NarQ (Pput_2149)	PP_2643	4HB	1,480 ± 500	161 ± 16	1 mM 4-HBA (21)
McfR-NarQ (Pput_0339)	PP_0317	4HB	1,640 ± 310	282 ± 72	1 mM malate (22)
McfS-NarQ (Pput_4520)	McpS (PP_4658)	HBM	1,210 ± 226	441 ± 89	1 mM malate (22)
McfQ-NarQ (Pput_4894)	McpQ (PP_5020)	HBM	1,460 ± 115	992 ± 118	1 mM citrate (22)
Pput_0342-NarQ (McfH)	McpH (PP_0320)	dCache	1,573 ± 186	778 ± 97	2 mM xanthine (32)
Pput_3489-NarQ (McfA)	McpA (PP_2249)	dCache	1,831 ± 153	664 ± 48	5 mM asparagine (51, 52)
Pput_4352-NarQ (McfG)	PctApp/McpG (PP_1371)	dCache	1,468 ± 224	323 ± 172	2 mM tryptophan (52)
Pput_1257-NarQ (McfU)	McpU (PP_1228)	dCache	2,540 ± 55	1,910 ± 95	10 mM propionate (this study[e])
Pput_2828-NarQ (McfP)	McpP (PP_2861)	sCache	3,140 ± 315	2,190 ± 270	10 mM pyruvate (77)
Pput_3459-NarQ (McfO)	PP_2310	Small unknown	970 ± 296	220 ± 20	10 mM propionate (this study[e])
Pput_2091-NarQ	NA	4HB	3,230 ± 1,240	NT	
Pput_4764-NarQ	PP_4888	SMP_2	1,120 ± 540	NT	
Pput_3892-NarQ	PP_1819	dCache	1,420 ± 230	NT	
McpC-NarQ	PP_0584	dCache	220 ± 40	470 ± 80	10 mM nicotinic acid (71)
Pput_2217-NarQ	PP_3557	dCache	97 ± 9	NT	
Pput_3621-NarQ	PP_2120	4HB	130 ± 30	NT	
Pput_4234-NarQ	PP_1488	4HB	121 ± 61	NT	
Pput_4895-NarQ	PP_5021	HBM	110 ± 25	NT	

[a]Unnamed MCPs are indicated by their Pput (strain F1) or PP (strain KT2440) locus tag numbers; Mcf names for *P. putida* F1 MCPs are now assigned based on the corresponding Mcp designations for functionally characterized *P. putida* KT2440 MCPs. NA, not applicable.
[b]4HB, 4-helix bundle; HBM, helical bimodular; sCache, single Cache; dCache, double Cache; SMP_2, a type of Cache domain found in *Proteobacteria* (14, 25, 42).
[c]Activities are in arbitrary (Miller) units. Averages and standard deviations from at least three independent replicates are shown. NT, not tested/ligand(s) unknown.
[d]References reporting ligands for *P. putida* F1 MCPs if known or for the KT2440 ortholog. 4-HBA, 4-hydroxybenzoate.
[e]Data are reported in "Functional screening of hybrid MCPs: identification of multiple receptors that sense propionate" in Results.

to those for the PcaY-mediated chemotactic responses of *P. putida* F1. Results of quantitative capillary assays indicated that quinate and shikimate were the strongest attractants and were sensed at the lowest concentrations (Fig. 5B). The peak chemotactic response of *P. putida* F1 to all attractants except vanillin was at 1 mM, and the minimum concentrations detected were below 100 μM (Fig. 5B). Although there was no binding detected between vanillin and the PcaY LBD in ITC experiments (Table 1), the PcaY-NarQ reporter responded to vanillin at a high concentration (10 mM), suggesting very weak binding of this attractant.

Analysis of 17 additional MCP-NarQHAMP hybrids. The *P. putida* F1 genome encodes 20 putative MCPs with the same general structure as that of *E. coli* MCPs: an N-terminal periplasmic LBD flanked by two transmembrane domains and a cytoplasmic signaling domain. Similar to the MCPs in *P. putida* KT2440 (25), the LBDs in *P. putida* F1 fall into both cluster I (120 to 210 amino acids) and cluster II (220 to 300 amino acids) and represent several different predicted domain types: 4-helix bundle (4HB), helical bimodular (HMB), three Cache variations (single Cache [sCache], double Cache [dCache], and SMP_2), and small unknown (Table 2) (14). To test whether additional hybrids with the same HAMP junction point would be functional, 17 hybrid receptors representing 6 different LBD types were constructed with junction points identical to that of the responsive PcaY-NarQ receptor. The ability of these hybrid receptors to autophosphorylate and transfer the phosphoryl group to NarL was tested by monitoring Φ(*narG-lacZ*) expression in *E. coli* VJS5054 in the absence of any added chemical ligands. β-Galactosidase activity was detected for VJS5054 carrying each of the hybrid receptors, and activities for most of them were comparable to or higher than that seen with the unstimulated PcaY-NarQ hybrid (Table 2). However, the Φ(*narG-lacZ*) expression level was unexpectedly low in VJS5054 carrying five of the hybrid receptors (McpC-NarQ, Pput_2217-NarQ, Pput_3621-NarQ, Pput_4234-NarQ, and Pput_4895-NarQ); β-galactosidase activities were comparable to those of unstimulated wild-type NarQ and 4-HBA-stimulated PcaY-NarQ (Table 2). One of these hybrid receptors (McpC) appeared to have a weak inverted response to the known ligand nicotinic acid (Table 2).

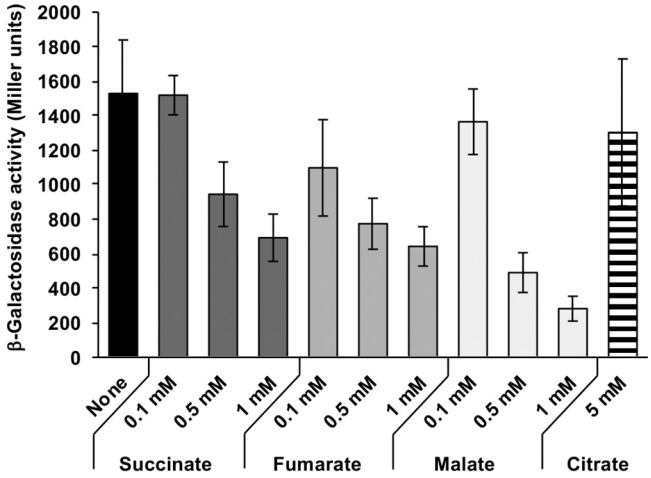

FIG 6 Φ(*narG-lacZ*) expression in *E. coli* VJS5054 carrying McpR-NarQ. β-Galactosidase assays were carried out on cultures grown with the indicated concentrations of succinate, fumarate, malate, and citrate. Results are averages from at least three independent experiments, with error bars representing standard deviations.

The others may also have inverted responses, but additional work will be needed to test this possibility, as there are currently no known ligands for these receptors. Nevertheless, representative hybrids with all six LBD types conferred Φ(*narG-lacZ*) expression at levels similar to that with unstimulated PcaY-NarQ (Table 2), demonstrating that they have kinase activity and can transphosphorylate NarL. In addition, ligand sensing and signaling by several hybrids for which ligands are known or predicted based on *P. putida* KT2440 MCP orthologs were demonstrated for one ligand each at a single concentration (Table 2). The results show signaling by hybrid receptors with five different LBD types.

Validation of concentration-dependent sensing and signaling by McfR-NarQ. Previous work in our laboratory demonstrated that the receptor encoded by *Pput_0339* (McfR) was responsible for chemotaxis to malate, fumarate, and succinate but not citrate (22); however, direct binding to attractants by McfR had not been demonstrated. To test the function and specificity of the McfR-NarQ receptor and to determine whether McfR binds ligands directly, we examined Φ(*narG-lacZ*) expression after growing *E. coli* VJS5054 carrying the McfR-NarQ hybrid construct in the presence and absence of organic acids. McfR-NarQ exhibited concentration-dependent responses to malate, fumarate, and succinate and no response to citrate, even at a high concentration (Fig. 6). The limit of detection for each compound was between 100 and 500 μM (Fig. 6). The sensitive and specific responses of the hybrid protein expressed in *E. coli* provide strong evidence that succinate, fumarate, and malate all bind directly to McfR.

Construction of a sensitive hybrid naphthalene biosensor. Using the same junction points as in the *P. putida* F1 MCP-NarQ hybrids, we constructed and tested a NahY-NarQ hybrid receptor. NahY is the naphthalene chemoreceptor from *P. putida* G7 (26); it is a cluster I receptor with a 4HB domain type predicted using Pfam 32.0 (27). The level of Φ(*narG-lacZ*) expression in the absence of the ligand suggested that the hybrid was functional, and sensitive concentration-dependent signaling was demonstrated when the reporter strain was grown in the presence of increasing concentrations of naphthalene (0.25 to 250 μM) (Fig. 7). These results are consistent with the demonstrated response to naphthalene concentrations of ~25 to 250 μM by *P. putida* G7 in quantitative capillary assays (28). The estimated binding affinity for naphthalene based on these data (see the plot in Fig. S3) was 513 ± 185 nM, which indicates that the hybrid receptor is a very sensitive biosensor for naphthalene.

Functional screening of hybrid MCPs: identification of multiple receptors that sense propionate. To test whether ligands could be identified for receptors of un-

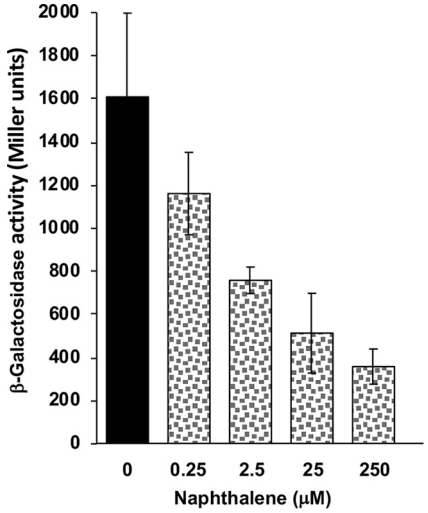

FIG 7 Φ(*narG-lacZ*) expression in *E. coli* VJS5054 carrying the NahY-NarQ hybrid reporter. β-Galactosidase assays were carried out on cultures grown with the indicated concentrations of naphthalene. Results are averages from at least three independent experiments, with error bars representing standard deviations.

known function by screening in *E. coli*, we carried out β-galactosidase assays with VJS5054 carrying each of the functional hybrid receptors after growth in the presence of propionate, which is a good carbon source and chemoattractant for *P. putida* F1. Surprisingly, after a quick series of β-galactosidase assays following growth in the presence and absence of 10 mM propionate, it appeared that six of the hybrid receptors responded to propionate, including McfR-NarQ, Pput_1257-NarQ, Pput_2828-NarQ, Pput_3459-NarQ, Pput_3489-NarQ, and Pput_4352-NarQ (data not shown). To confirm the results of the screen, we tested a range of propionate concentrations (1, 5, and 10 mM) and found that the Pput_3459-NarQ and Pput_2828-NarQ hybrids were the most sensitive, clearly responding to 1 mM propionate. Pput_1257-NarQ was the least sensitive, responding only weakly to 10 mM propionate. McfR-NarQ, Pput_3489-NarQ, and Pput_4352-NarQ showed intermediate responses, detecting 5 mM propionate (Fig. 8). As a negative control, we tested Φ(*narG-lacZ*) expression in VJS5054 carrying PcaY-NarQ with and without 10 mM propionate. Results of LacZ assays were 1,690 ± 240 and 1,620 ± 320 Miller units in the absence and presence of 10 mM

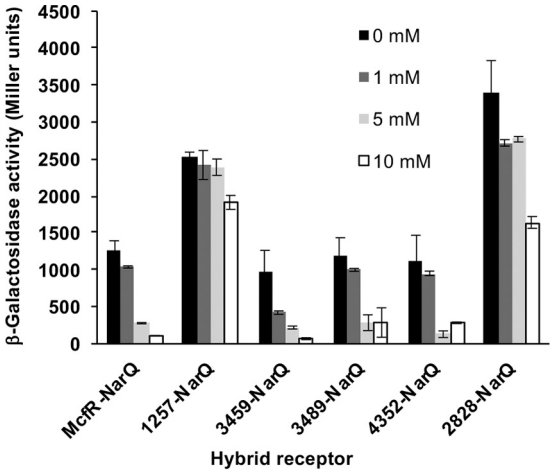

FIG 8 Φ(*narG-lacZ*) expression in *E. coli* VJS5054 carrying six different MCP-NarQ hybrid receptors in response to propionate. β-Galactosidase assays were carried out on cultures grown with the indicated concentrations of propionate. Results are averages from at least three independent experiments, with error bars representing standard deviations.

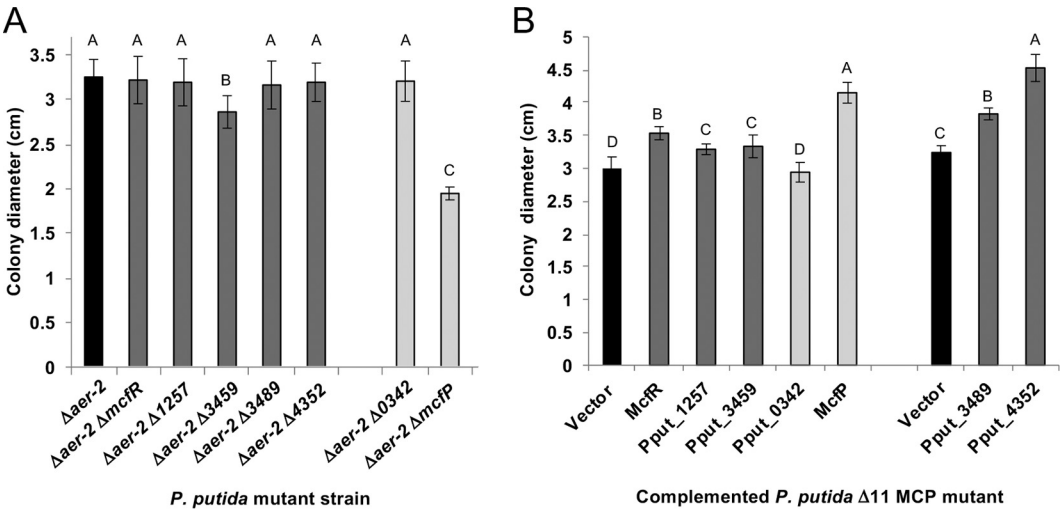

FIG 9 Chemotactic responses of *P. putida* mutants to 1 mM propionate in quantitative swim plate assays. (A) Responses of the *P. putida* F1 Δ*aer-2* deletion mutant (black bar, control) were compared to those of double mutants lacking *aer-2* and each of the putative propionate receptor genes identified in the MCP-NarQ hybrid reporter screen (gray bars, strains listed in Table 3). The Δ*aer-2* Δ*mcfP* mutant (light-gray bar on the far right) is the ortholog of the *P. putida* KT2440 propionate chemoreceptor. The Δ*aer-2* Δ*Pput_0342* mutant (light-gray bar) was not expected to respond to propionate based on the absence of a response of the *E. coli* reporter strain carrying the Pput_0342-NarQ hybrid to propionate. (B) Responses of the *P. putida* F1Δ11 deletion mutant RPF018 harboring either the empty vector pRK415 or pRK415Km (black bars) were compared to those of strains carrying the indicated wild-type MCP genes in the respective vectors (plasmid names listed in Table 4). The gray bars represent complementation of propionate chemotaxis with the receptors identified in the hybrid receptor propionate screen. The light-gray bars represent complementation with *Pput_0342* (not expected to complement) and *mcfP* (expected to complement). Results are averages from at least three independent experiments, with error bars representing standard deviations. Means with the same letter are not significantly different ($P < 0.05$ by one-way analysis of variance [ANOVA] with a Tukey multiple-comparison test).

propionate, respectively. These results indicate that responses to propionate are specific to a subset of *P. putida* MCPs. When this study was initiated, no receptors for propionate had been identified; however, an MCP for propionate from *P. putida* KT2440 (McpP) has since been reported (25). McpP corresponds to Pput_2828 in *P. putida* F1 (99% amino acid sequence identity; designated McfP here).

Chemotaxis assays with mutants verify a role for the six receptors in mediating the response to propionate. To test whether each of the six MCPs identified in the hybrid receptor screen contributes to the chemotactic response of *P. putida* F1 to propionate, we carried out quantitative swim plate assays with strains each lacking one of the putative propionate receptors in a Δ*aer-2* mutant background since energy taxis has been shown to mask chemotaxis phenotypes in this assay (22, 29). As expected, the Δ*aer-2* Δ*mcfP* double mutant showed a clear defect in the response to propionate (Fig. 9A, right), indicating that the McpP ortholog in *P. putida* F1 is capable of sensing propionate. We also tested the chemotactic response of the Δ*aer-2* Δ*Pput_0342* mutant of *P. putida* F1 to propionate. The Pput_0342-NarQ hybrid receptor from *P. putida* F1 did not respond to 10 mM propionate in initial β-galactosidase screens (data not shown), so the Δ*Pput_0342* mutant strain was used as a negative control. As expected, the Δ*aer-2* Δ*Pput_0342* mutant did not have a defect in propionate chemotaxis compared to the Δ*aer-2* control strain (Fig. 9A, right). Consistent with the Pput_3459-NarQ hybrid reporter data, the Δ*aer-2* Δ*Pput_3459* mutant strain showed a significant defect in the chemotaxis response to propionate, while the Δ*aer-2* Δ*mcfR*, Δ*aer-2* Δ*Pput_1257*, Δ*aer-2* Δ*Pput_3489*, and Δ*aer-2* Δ*Pput_4352* mutants behaved like the Δ*aer-2* control strain (Fig. 9A, left).

Since four of the deletion mutants lacking single putative propionate MCP genes (Δ*mcfR*, Δ*Pput_1257*, Δ*Pput_3489*, and Δ*Pput_4352*) did not show obvious defects in chemotaxis assays, we utilized a mutant strain in which 11 of the 20 putative genes encoding canonical MCPs in *P. putida* F1 had been deleted (F1Δ11) (Table 3). Genes encoding the six putative propionate MCPs identified in the MCP hybrid screen with

TABLE 3 Bacterial strains used in this study

Strain	Relevant characteristic(s)	Reference(s) or source
E. coli		
BL21(DE3)	Protein production strain	72
DH5α	Cloning host	Life Technologies, Gaithersburg, MD
DH5α λ*pir*	Cloning host	William W. Metcalf
HB101	Host for mobilization plasmid pRK2013	56
VJS5054	$\lambda\Phi$(*narG-lacZ*)*250* Δ(*argF-lac*)*U169* Δ*narX242 narQ251*::Tn*10*d(Tc) *pcnB1 zad-981*::Tn*10*d(Km)	5
P. putida		
F1	Wild-type toluene-degrading strain	73, 74
GC005	F1 Δ*aer-2* Δ*Pput_0342* (*mcfH*)	This study
GC006	F1 Δ*aer-2* Δ*pcaY*	21
GC007	F1 Δ*aer-2* Δ*Pput*_2828 (*mcfP*)	This study
GC008	F1 Δ*aer-2* Δ*Pput*_3459 (*mcfO*)	This study
GC010	F1 Δ*aer-2* Δ*Pput*_3489 (*mcfA*)	This study
GC012	F1 Δ*aer-2* Δ*Pput*_4352 (*mcfG*)	This study
GC013	F1 Δ*aer-2* Δ*Pput*_1257 (*mcfU*)	This study
GC021	F1 Δ*aer-2* Δ*mcfR*	22
GC104	F1 Δ*Pput_3489* Δ*Pput_4352* Δ*mcpC*	This study
GC105	F1 Δ*Pput_3489* Δ*Pput_4352* Δ*mcpC* Δ*mcfR*	This study
G7	Wild-type naphthalene-degrading strain	75
RPF010	F1 Δ*Pput_3489* Δ*Pput_4352* Δ*mcpC* Δ*mcfR* Δ*mcfQ*	This study
RPF011	F1 Δ*Pput_3489* Δ*Pput_4352* Δ*mcpC* Δ*mcfR* Δ*mcfQ* Δ*mcfS*	This study
RPF014	F1 Δ*Pput_3489* Δ*Pput_4352* Δ*mcpC* Δ*mcfR* Δ*mcfQ* Δ*mcfS* Δ*Pput_0342*	This study
RPF015	F1 Δ*Pput_3489* Δ*Pput_4352* Δ*mcpC* Δ*mcfR* Δ*mcfQ* Δ*mcfS* Δ*Pput_0342* Δ*pcaY*	This study
RPF016	F1 Δ*Pput_3489* Δ*Pput_4352* Δ*mcpC* Δ*mcfR* Δ*mcfQ* Δ*mcfS* Δ*Pput_0342* Δ*pcaY* Δ*Pput_4234*	This study
RPF017	F1 Δ*Pput_3489* Δ*Pput_4352* Δ*mcpC* Δ*mcfR* Δ*mcfQ* Δ*mcfS* Δ*Pput_0342* Δ*pcaY* Δ*Pput_4234* Δ*Pput_4764*	This study
RPF018 (F1Δ11)	F1 Δ*Pput_3489* Δ*Pput_4352* Δ*mcpC* Δ*mcfR* Δ*mcfQ* Δ*mcfS* Δ*Pput_0342* Δ*pcaY* Δ*Pput_4234* Δ*Pput_4764* Δ*Pput_3459*	This study
XLF002	F1 Δ*Pput_0342* (*mcfH*)	This study
XLF006	F1 Δ*Pput_1257* (*mcfU*)	This study
XLF010	F1 Δ*PcaY*	21
XLF014	F1 Δ*Pput_2828* (*mcfP*)	This study
XLF015	F1 Δ*Pput_3459* (*mcfO*)	This study
XLF017	F1 Δ*Pput_3489* (*mcfA*)	This study
XLF019	F1 Δ*aer-2*	65
XLF022	F1 Δ*Pput_4352* (*mcfG*)	This study
XLF128	F1 Δ*Pput_3489* Δ*Pput_4352*	This study

propionate as well as that encoding Pput_0342 were individually expressed in F1Δ11, and the responses of these complemented strains were tested in swim plate assays. As expected, the presence of *Pput_0342* had no effect on the response to propionate, whereas when complemented with *mcfR*, *Pput_1257*, *Pput_3459*, *Pput_3489*, or *Pput_4352*, the F1Δ11 mutant showed significantly stronger responses to propionate than the control strains carrying the vector only (Fig. 9B). In addition, even though the F1Δ11 mutant carries an intact copy of *mcfP*, the presence of additional copies of *mcfP* on pRK415Km increased the response to propionate. Together, these findings indicate that *P. putida* F1 has six MCPs that participate in chemotaxis to propionate, although clearly, the major contributors are Pput_2828 (McfP) and, to a lesser extent, Pput_3459 (designated McfO here).

DISCUSSION

Strategies for functional characterization of MCPs. There has been a recent push to develop higher-throughput methods for the characterization of MCPs of unknown function, given that there are technical and functional limitations to traditional methods (30). Genetic approaches, such as the generation of chemoreceptor mutants, can be difficult depending on the bacterial species and whether the strain of interest is amenable to genetic manipulation. In many cases, MCPs are functionally redundant, which can mask the phenotype of single mutants (16), which was the case with propionate detection by *P. putida* F1 as shown here. Recently, a fluorescence-based

thermal shift assay was developed to rapidly link the LBDs of MCPs to their ligands (31). In this assay, the binding affinity of an attractant for a purified LBD can be measured based on the fluorescence increase as a result of the binding of fluorescent dye to the protein during thermal unfolding. Those researchers were able to survey up to 95 potential ligands at once using 96-well plates and in this way characterized the ligand-binding profiles of three putative amino acid chemoreceptors in *Pseudomonas syringae*. A similar assay resulted in the identification of the chemoreceptor McpH for purines and its derivatives in *P. putida* KT2440 (32, 33). However, it is not always trivial to purify stable, correctly folded LBDs for use in these types of screens (33), and in some cases, inhibitors of chemotaxis have been shown to bind to LBDs (34). The use of hybrid receptors provides an alternative strategy to screen for receptor-ligand binding that circumvents these potential issues.

The construction of hybrid two-component receptors is not new, as previous studies have reported hybrid *E. coli* MCPs (35–37), hybrid *E. coli-Pseudomonas* MCPs (38), and hybrids between MCPs and other two-component sensors (19, 20), among others. A variation of our strategy has been used to develop novel biosensors using fluorescence resonance energy transfer (FRET) to monitor the phosphorylation-dependent interaction of CheY with CheZ via their fluorescent fusion protein derivatives in response to ligand sensing by hybrid MCPs (39). In that study, hybrid chemoreceptors with various LBD types were also shown to be functional, and screening for new ligands was carried out using a FRET-based microfluidic assay.

PcaY binds attractants directly. In this study, we used a chemotaxis-independent β-galactosidase reporter system to demonstrate that the PcaY LBD binds directly to the known attractants sensed by PcaY via *P. putida* F1. The hybrid receptor could differentiate between structurally similar aromatic chemicals, and LacZ activity levels decreased in response to increasing ligand concentrations. In previous studies, we were unable to rule out the possibility that PcaY could be sensing downstream metabolites of some of the attractants in *P. putida* F1 (21), as was shown to be the case for aromatic acid sensing by *Comamonas testosteroni* (34, 40). The results obtained using the PcaY-NarQ hybrid clearly demonstrate that the hydroaromatic compounds quinate and shikimate and the various substituted benzoates are directly bound by the LBD of PcaY, and these results are consistent with the results of our ITC experiments as well as those with the *P. putida* KT2440 ortholog of PcaY (24). In addition, binding affinities estimated from the *in vivo* β-galactosidase data provide good approximations of the binding constants obtained in ITC experiments (Table 1). Finally, our results suggest that the PcaY-NarQ hybrid detected vanillin at a high concentration (10 mM), despite the lack of binding in ITC experiments, which could indicate that vanillin, rather than a metabolite, binds the PcaY LBD directly albeit with low affinity. This finding suggests that the use of hybrid receptors may be more sensitive than *in vitro* binding assays.

A single junction point yields functional hybrids with a high success rate. The inclusion of the native HAMP domain from NarQ was crucial to the functionality of the hybrid receptor. HAMP domains have conserved motifs, including two predicted amphiphilic helices (AS1 and AS2) joined by a nonhelical connector. The hydrophobicity of the amphiphilic helices is critical for the packing interactions of HAMP (10). Hybrids in which AS1 from one protein was fused to AS2 from another protein were nonfunctional (3). Moreover, studies showed that truncation or deletion of AS1 and AS2 of NarX and NarQ caused significant changes in protein function and often had deleterious effects (3). These studies also showed that constructs in which the entire HAMP region of NarX was replaced also resulted in nonfunctional NarX hybrids, and similarly, a NarX-Tar hybrid that contained the NarX HAMP domain was also functional (19). For these reasons, we did not include a construct in which PcaY was linked to NarX via the PcaY HAMP domain.

At this time, we do not fully understand the reasons why some of the constructed hybrids appeared to be in a constitutively "off" state, but hybrid receptors with a range of phenotypes have been reported previously. For example, construction of hybrids

between the *E. coli* Tar chemoreceptor and the osmosensor histidine kinase EnvZ resulted in functional hybrids that were responsive to aspartate, an attractant that binds Tar directly, as well as hybrids that were constitutively "on" or constitutively "off" (18). The packing stability of the HAMP domain is highly critical to signaling (10), so any displacement of its structural integrity could have resulted in a nonfunctional sensory protein. In addition, the region immediately upstream of the HAMP domain, termed the control cable, is critical for proper signaling (41). However, inspection of the control cable and the second transmembrane helix (TM2) sequences in the *P. putida* MCPs did not reveal control cable (or TM2) features that explain the different signaling responses of different hybrid receptors (see Fig. S4 in the supplemental material).

Extensive mutational analysis of various Tar-EnvZ hybrids demonstrated that a single point mutation in the HAMP domain of a ligand-blind receptor hybrid Tar-EnvZ receptor could convert it to one capable of sensing aspartate, and the insertion of two amino acid residues near the junction of the transmembrane and HAMP domains could convert a receptor from constitutively "on" to constitutively "off" (18). It is therefore likely that random mutagenesis and screening for higher β-galactosidase activity on MacConkey plates or plates containing X-Gal (5-bromo-4-chloro-3-indolyl-β-D-galactopyranoside) as described in the Tar-EnvZ studies (18) would allow us to isolate functional variants of our constitutively "off" hybrids. However, the 74% success rate for constructing hybrids capable of signaling using a single set of junction points validates the use of this strategy for characterizing LBD function.

Hybrids with diverse LBDs are functional. Genome analyses have revealed that the LBD structures of MCPs are very diverse across bacterial and archaeal species. The high level of sequence divergence between the LBDs makes predicting attractant profiles based on sequence comparisons challenging. MCPs have been cataloged into two clusters based on LBD size and domain structure similarities (11). The LBDs of MCPs that fall into cluster I, such as PcaY, are typically between 120 and 210 amino acids in size, and they form a 4-helix bundle (4HB), single CACHE (sCache), or a small unknown structure, whereas those in cluster II are between 220 and 300 amino acids in size and form a helical bimodular (HBM), double Cache (dCache), or SMP_2 (another Cache variation) structure (11, 14, 42). Importantly, LBDs with completely different predicted structures have been shown to bind the same or similar ligands. For example, the *P. putida* receptors McfQ, McfS, and McfR all detect fumarate, yet their LBDs have little sequence conservation, and although McfS and McfQ have HBM domain structures, McfR is predicted to have a 4HB domain (22). Similarly, the *P. putida* receptors McpS and McpP both bind acetate and have different predicted domain structures (25, 43). Hybrids constructed from LBDs with all known types of *Pseudomonas* LBD structures (4HB, HBM, sCache, dCache, SMP_2, and small unknown) were capable of signaling (Table 2), and 10 of the functional receptors (representing five different LBD structures) were shown to respond to one or more ligands. Based on these results, we anticipate that the general design of our PcaY-NarQ hybrid can be utilized to identify the range of ligands bound by any MCP from any bacterial species or even from metagenomic sequence data.

Analysis of hybrid sensors in the *E. coli* reporter strain VJS5054, in which the *lacZ* operon is under the control of the nitrate-responsive *narG* promoter, provides a rapid and simple assay that can be used to identify MCP function by screening for potential attractants in *E. coli*. This design allowed sensitive and specific detection of the type and amount of ligand present and could be used to estimate ligand binding affinity. In previous studies, chemoreceptors with altered specificity were generated (20, 39, 44–47). Hybrid receptors could be used to rapidly screen for specificity changes following targeted or random mutagenesis of the LBD-encoding DNA fragment. In addition, hybrid receptors such as the NahY-NarQ receptor have the potential to be useful as biosensors, and construction of modified MCPs should allow one to design new biosensors and/or alter the chemosensory repertoire of any motile bacterial strain.

One caveat to identifying ligands using either hybrid receptors or *in vitro* binding assays is in the case of attractants that bind to periplasmic binding proteins. In this case, the attractant/periplasmic binding protein complex interacts with a specific MCP, as is the case with chemotaxis to sugars, dipeptides, and AI-2 by *E. coli* (13, 48, 49) and sensing of inorganic phosphate in *Pseudomonas aeruginosa* by the MCP CtpL via the periplasmic binding protein CtpS (50). However, it is possible that screening could be carried out with a reporter strain in which the binding protein gene is expressed in addition to the hybrid MCP gene.

Functions of the multiple propionate receptors. One surprising finding, especially in light of the characterization of a single propionate chemoreceptor, McpP, in *P. putida* KT2440, is the presence of six different chemoreceptors that contribute to the response to propionate in *P. putida* F1. Homologs of all six receptors that are 97 to 99% identical to the *P. putida* F1 chemoreceptors are present in strain KT2440, so they are likely to have similar functions in both strains. The identification of six receptors capable of binding propionate would have been difficult using standard mutant screening and possibly even by *in vitro* binding assays with purified LBDs. This result highlights the sensitivity of the use of hybrid receptors to identify the ligands.

McfP, the primary propionate receptor and the ortholog of McpP from strain KT2440 (25), also senses lactate, acetate, and pyruvate (Table 2) (77). Although the McfP-NarQ hybrid detected propionate, it was not as sensitive to this ligand as would be expected based on the obvious defect in the chemotaxis response to propionate by the *P. putida* F1 McfP mutant (Fig. 9A) and the K_d of the McpP LBD from KT2440 (34 μM) (25). The reason for the weak response of the McfP-NarQ hybrid to both propionate (Fig. 8) and pyruvate (Table 2) is not known at this time, but the LacZ activity of the unstimulated McfP-NarQ hybrid was significantly higher than those of the other hybrids. It is therefore possible that the conformation of this hybrid is strongly poised to autophosphorylate and that the addition of the ligand only slightly affects its balance between kinase and phosphatase activities.

Based on the results of chemotaxis assays with mutant strains (Fig. 9A), Pput_3459 (McfO) appears to make a significant contribution to the response to propionate. Currently, there are no other known ligands for McfO, which is predicted to have a small LBD of unknown structure. Although increased responses to propionate were detected when the other four receptors were overexpressed in the Δ11 mutant (Fig. 9B), no obvious defects were seen for single-deletion mutants (Fig. 9A). Therefore, the contributions of these receptors may not be physiologically relevant in the wild-type strain, which highlights the importance of directly testing chemotaxis responses in the appropriate mutant backgrounds in addition to screening using hybrid receptors. Each of these minor propionate receptors has been shown to be important for sensing other attractants. McfR senses malate, succinate, and fumarate (22), and the receptor encoded by *Pput_3489* (McfA) and its KT2440 ortholog sense amino acids (51–53). In addition, the KT2440 orthologs of Pput_1257 (McpU) and Pput_4352 (PctApp/McpG) sense polyamines (53) and amino acids and gamma-aminobutyrate (38, 54), respectively. Binding to some of the known ligands for the other propionate receptors was confirmed here using the hybrid receptors (Table 2).

In conclusion, the construction and analysis of hybrid MCPs provide an additional strategy to identify chemoreceptor function that complements other currently available methods. The detection method used, which is independent of the chemotaxis system, provides an accurate measurement of ligand binding. Advantages include high sensitivity and simplicity of analysis (i.e., no major equipment is needed), and the demonstration that functional hybrids can be generated with a wide range of LBD types suggests that this method should be broadly applicable regardless of the source of the MCP.

MATERIALS AND METHODS

Bacterial strains, plasmids, and primers. Bacterial strains and plasmids used in this study are listed in Tables 3 and 4, respectively. Primers used in this study are shown in Table S1 in the supplemental

TABLE 4 Plasmids used in this study

Plasmid	Relevant characteristics[a]	Reference or source
pAW19	*sacB*-containing suicide vector; Ap^r Km^r	62
pET28a(+)	His tag expression vector; Km^r	Novagen
pET28b(+)	His tag expression vector; Km^r	EMD Millipore
pET28b-PcaY-LBD	Plasmid for expression and purification of the PcaY LBD; Km^r	This study
pGCF101	*Pput_0339* (*mcfR*) cloned into pRK415Km; Km^r	22
pGCF102	*Pput_0342* (*mcfH*) cloned into pRK415Km; Km^r	This study
pGCF106	*Pput_1257* (*mcfU*) cloned into pRK415Km; Km^r	This study
pGCF114	*Pput_2828* (*mcfP*) cloned into pRK415Km; Km^r	This study
pGCF115	*Pput_3459* (*mcfO*) cloned into pRK415Km; Km^r	This study
pJPF001	LBD-coding sequence of *Pput_0339* (*mcfR*) fused with cytoplasmic and HAMP domain-coding sequences of *narQ* in pHG165; Ap^r	This study
pJPF002	LBD-coding sequence of *Pput_0342* (*mcfH*) fused with cytoplasmic and HAMP domain-coding sequences of *narQ* in pHG165; Ap^r	This study
pJPF004	LBD-coding sequence of *Pput_0623* (*mcpC*) fused with cytoplasmic and HAMP domain-coding sequences of *narQ* in pHG165; Ap^r	This study
pJPF006	LBD-coding sequence of *Pput_1257* (*mcfU*) fused with cytoplasmic and HAMP domain-coding sequences of *narQ* in pHG165; Ap^r	This study
pJPF009	LBD-coding sequence of *Pput_2091* fused with cytoplasmic and HAMP domain-coding sequences of *narQ* in pHG165; Ap^r	This study
pJPF011	LBD-coding sequence of *Pput_2217* fused with cytoplasmic and HAMP domain-coding sequences of *narQ* in pHG165; Ap^r	This study
pJPF014	LBD-coding sequence of *Pput_2828* (*mcfP*) fused with cytoplasmic and HAMP domain-coding sequences of *narQ* in pHG165; Ap^r	This study
pJPF015	LBD-coding sequence of *Pput_3459* (*mcfO*) fused with cytoplasmic and HAMP domain-coding sequences of *narQ* in pHG165; Ap^r	This study
pJPF017	LBD-coding sequence of *Pput_3489* (*mcfA*) fused with cytoplasmic and HAMP domain-coding sequences of *narQ* in pHG165; Ap^r	This study
pJPF018	LBD-coding sequence of *Pput_3621* fused with cytoplasmic and HAMP domain-coding sequences of *narQ* in pHG165; Ap^r	This study
pJPF020	LBD-coding sequence of *Pput_3892* fused with cytoplasmic and HAMP domain-coding sequences of *narQ* in pHG165; Ap^r	This study
pJPF021	LBD-coding sequence of *Pput_4234* fused with cytoplasmic and HAMP domain-coding sequences of *narQ* in pHG165; Ap^r	This study
pJPF022	LBD-coding sequence of *Pput_4352* fused with cytoplasmic and HAMP domain-coding sequences of *narQ* in pHG165; Ap^r	This study
pJPF023	LBD-coding sequence of *Pput_4520* (*mcfS*) fused with cytoplasmic and HAMP domain-coding sequences of *narQ* in pHG165; Ap^r	This study
pJPF024	LBD-coding sequence of *Pput_4764* fused with cytoplasmic and HAMP domain-coding sequences of *narQ* in pHG165; Ap^r	This study
pJPF026	LBD-coding sequence of *Pput_4894* (*mcfQ*) fused with cytoplasmic and HAMP domain-coding sequences of *narQ* in pHG165; Ap^r	This study
pJPF027	LBD-coding sequence of *Pput_4895* fused with cytoplasmic and HAMP domain-coding sequences of *narQ* in pHG165; Ap^r	This study
pJPG001	LBD-coding sequence of *nahY* fused with cytoplasmic and HAMP domain-coding sequences of *narQ* in pHG165; Ap^r	This study
pPYNQ1	LBD-coding sequence of *pcaY* fused with cytoplasmic and HAMP domain-coding sequences of *narQ* in pHG165; Ap^r	This study
pPYNQ2	LBD- and HAMP domain-coding sequences of *pcaY* fused with the cytoplasmic coding sequence of *narQ* in pHG165; Ap^r	This study
pPYNQ3	LBD- and HAMP domain-coding sequences of *pcaY* fused with the cytoplasmic coding sequence of *narQ* in pHG165; contains a codon change at position 222 from Leu to Gln; Ap^r	This study
pPYX1	LBD-coding sequence of *pcaY* fused with cytoplasmic and HAMP domain-coding sequences of *narX* in pHG165; Ap^r	This study
pRK415	Broad-host-range cloning vector; Tc^r	66
pRK415Km	Broad-host-range cloning vector; Km^r	65
pRK2013	ColE1 *ori*; RP4 mobilization function; Km^r	76
pVJS3353	*narX* in pHG165; Ap^r	3
pVJS3354	*narQ* in pHG165; Ap^r	3
pXLF001	*Pput_0339* (*mcfR*) upstream and downstream 1-kb PCR fragments fused and cloned into SpeI-SacI sites of pAW19; Ap^r Km^r	22
pXLF002	*Pput_0342* (*mcfH*) upstream and downstream 1-kb PCR fragments fused and cloned into SpeI-SacI sites of pAW19; Ap^r Km^r	This study
pXLF004	*Pput_0623* (*mcpC*) upstream and downstream 1-kb PCR fragments fused and cloned into SpeI-SacI sites of pAW19; Ap^r Km^r	68
pXLF006	*Pput_1257* (*mcfH*) upstream and downstream 1-kb PCR fragments fused and cloned into SpeI-SacI sites of pAW19; Ap^r Km^r	This study
pXLF010	*Pput_2149* (*pcaY*) upstream and downstream 1-kb PCR fragments fused and cloned into SpeI-SacI sites of pAW19; Ap^r Km^r	21
pXLF014	*Pput_2828* (*mcfP*) upstream and downstream 1-kb PCR fragments fused and cloned into the SpeI site of pAW19; Ap^r Km^r	This study
pXLF015	*Pput_3459* (*mcfO*) upstream and downstream 1-kb PCR fragments fused and cloned into SpeI-SacI sites of pAW19; Ap^r Km^r	This study
pXLF017	*Pput_3489* (*mcfA*) upstream and downstream 1-kb PCR fragments fused and cloned into SpeI-SacI sites of pAW19; Ap^r Km^r	This study
pXLF019	*Pput_3628* (*aer-2*) upstream and downstream 1-kb PCR fragments fused and cloned into SpeI-SacI sites of pAW19; Ap^r Km^r	65
pXLF021	*Pput_4234* upstream and downstream 1-kb PCR fragments fused and cloned into SpeI-SacI sites of pAW19; Ap^r Km^r	This study
pXLF022	*Pput_4352* (*mcfG*) upstream and downstream 1-kb PCR fragments fused and cloned into SpeI-SacI sites of pAW19; Ap^r Km^r	This study
pXLF023	*Pput_4520* (*mcfS*) upstream and downstream 1-kb PCR fragments fused and cloned into SpeI-SacI sites of pAW19; Ap^r Km^r	22
pXLF024	*Pput_4764* upstream and downstream 1-kb PCR fragments fused and cloned into SpeI-SacI sites of pAW19; Ap^r Km^r	This study
pXLF026	*Pput_4894* (*mcfQ*) upstream and downstream 1-kb PCR fragments fused and cloned into SpeI-SacI sites of pAW19; Ap^r Km^r	22
pXLF210	*pcaY* cloned into pRK415Km; Km^r	21
pXLF217	*Pput_3489* (*mcfA*) cloned into pRK415; Tc^r	This study
pXLF222	*Pput_4352* (*mcfG*) cloned into pRK415; Tc^r	This study

[a]Ap^r, ampicillin resistance; Km^r, kanamycin resistance; Tc^r, tetracycline resistance.

material. *E. coli* strains DH5α and DH5α λ*pir* were used for cloning and plasmid propagation. *E. coli* BL21(DE3) was used for expression and purification of the PcaY LBD. *E. coli* VJS5054 (5), which has null alleles of the *narX* and *narQ* genes and carries an Fnr- and NarL-responsive *narG-lacZ* operon fusion, was used as the reporter strain for analyzing the output of the hybrid receptors. Anerobic growth permits Fnr activation of expression from the *narG* promoter (2). Complementation with a plasmid-encoded *nar* sensor (NarX, NarQ, or an MCP-NarQ hybrid) permits further NarL-dependent activation of expression from the *narG* promoter under appropriate conditions. Strain VJS5054 also carries a *pcnB* mutation, which decreases the copy number of ColE1 plasmids carrying the hybrid constructs, to approximately 1 per cell (5, 55).

Culture media and growth conditions. *E. coli* strains were maintained on lysogeny broth agar at 37°C (56), and 200 μg ml^{-1} of ampicillin, 100 μg ml^{-1} of kanamycin, or 15 μg ml^{-1} of tetracycline was added for plasmid selection and maintenance. *E. coli* VJS5054 cultures were grown for LacZ assays as previously described (57, 58), with slight modifications. Briefly, strains were inoculated in phosphate-buffered minimal medium (MSB) (59) containing 80 mM glucose and 50 μg ml^{-1} ampicillin and grown aerobically overnight at 37°C. These cultures were used to inoculate 13-ml screw cap tubes filled to capacity with the same medium, with and without attractant chemicals added, as indicated. Cultures were grown anaerobically in a 37°C water bath until mid-exponential phase (optical density at 600 nm [OD_{600}] of between 0.3 and 0.4).

Cloning and DNA manipulations. *P. putida* F1 genomic DNA was isolated using the ArchivePure DNA kit (5 PRIME, Inc., Gaithersburg, MD). PCR products and plasmids were purified using a gel extraction kit (Bio Basic, Inc., Markham, Ontario, Canada) and a plasmid miniprep kit from Fermentas (Glen Burnie, MD), respectively. Restriction endonucleases and DNA modification enzymes were purchased from New England Biolabs (Beverly, MA). Standard procedures for *E. coli* transformation and the manipulation of plasmids and DNA fragments were followed (56). Sequences of all cloned PCR products were verified at the University of California, Davis, Sequencing Facility using fluorescence automated DNA sequencing with an Applied Biosystems 3730 automated sequencer.

Construction of an expression plasmid for the PcaY LBD. The DNA fragment encoding the LBD of PcaY (residues 35 to 184) was amplified by PCR using genomic DNA of *P. putida* F1 and primers YLBD-NdeI-F and YLBD-HindIII-R. The resulting product was digested and cloned into pET28a (Table 4). The insert and flanking regions of the resulting plasmid, pET28a-PcaY-LBD, were verified by DNA sequencing.

Purification of the PcaY LBD. *E. coli* BL21(DE3)(pET28a-PcaY-LBD) was grown in three 3-liter flasks, each containing 1 liter of LB medium supplemented with 50 μg/ml kanamycin, at 30°C. When the cultures reached an OD_{600} of 0.5, the growth temperature was lowered to 18°C, and expression was induced by the addition of 0.1 mM isopropyl-β-D-thiogalactopyranoside. Growth was continued at 18°C overnight (~12 h) prior to harvesting of cells by centrifugation at 6,000 $\times$ *g*. Cell pellets were resuspended in 50 ml of buffer A (20 mM Tris-HCl, 0.1 mM EDTA, 500 mM NaCl, 10 mM imidazole, 5% [vol/vol] glycerol [pH 7.8]) and broken by ultrasonication (200 W). The resulting lysate was subjected to centrifugation at 12,500 $\times$ *g* for 30 min. The supernatant was passed through a 0.45-μm-cutoff filter (Minisart) and loaded onto a 5-ml HisTrap HP column equilibrated with buffer A. Protein was eluted by applying a gradient of 45 mM to 500 mM imidazole in buffer A. Fractions were examined by SDS-PAGE, and the presence of the PcaY LBD was confirmed by determination of the molecular mass. Protein concentrations were determined by the Bradford assay (60).

Isothermal titration calorimetry. Isothermal titration calorimetry (ITC) measurements were conducted at 25°C using a Nano ITC 2G instrument (TA Instruments, Newcastle, DE, USA) with a 1-ml sample cell. The PcaY LBD was dialyzed twice against polybuffer [5 mM Tris-HCl, 5 mM piperazine-*N*,*N*′-bis(2-ethanesulfonic acid) (PIPES), 5 mM morpholineethanesulfonic acid (MES), 5 mM NaCl (pH 7.8)]. Protein at concentrations of 50 to ~110 μM was titrated with 2.5-μl aliquots of the ligand (0.5 or 1 mM in polybuffer) with stirring at 75 rpm. No precipitate was observed after titration was complete. Data were analyzed with the NanoAnalyze software package (TA Instruments, Newcastle, DE, USA).

Construction of *pcaY-nar* gene hybrids. Each hybrid construct was made using a total of three overlapping DNA fragments amplified using primers listed in Table S1 and then cloned into either pVJS3353 or pVJS3354 using an In-Fusion HD cloning kit (Clontech, Mountain View, CA). To construct PcaY-NarQHAMP, the DNA encoding the PcaY LBD region was amplified using primers 2149_narQ_For and 2149_narQ_Rev. An approximately 570-bp fragment encompassing the NarQ HAMP region and a portion of the C terminus was amplified using primers narQ_HAMP_For and narQ_ADAP_Rev. A third fragment containing overlapping sequences with pVJS3354 was amplified using primers pHG165_Eco_For and narQ_Eco_Rev. All three DNA fragments were gel purified using a commercially available gel extraction kit (Bio Basic, Inc., Markham, Ontario, Canada). The vector pVJS3354, which contains the full-length *narQ* gene, was digested with EcoRI and SacI to release a 1.8-kb DNA fragment containing the LBD and HAMP region of NarQ. All three amplicons were then directionally cloned into the EcoRI and SacI sites on digested pVJS3354. The hybrids PcaYHAMP-NarQ, PcaYHAMP-NarQ^{L222Q}, and PcaY-NarXHAMP were constructed similarly using primers listed in Table S1, and the amplicons were directionally cloned into pVJS3354, except for PcaY-NarXHAMP, which was cloned into pVJS3353. The resulting plasmids were introduced into VJS5054 by transformation (61).

Construction of additional MCP-NarQHAMP hybrids. Eighteen additional MCP-NarQHAMP hybrids with the same junction points as the PcaY-NarQHAMP hybrid were constructed using the In-Fusion HD cloning kit with vector pVJS3354 (Table 4) and primers listed in Table S1. Seventeen of these were MCPs from *P. putida* F1, and one was NahY from *P. putida* G7 (26).

Construction of *P. putida* F1 MCP deletion mutants. MCP deletion mutants in F1 were constructed using the suicide vector pAW19 (Table 4), which carries a kanamycin resistance gene and the *sacB* gene that confers sucrose sensitivity (62). The 1-kb regions upstream and downstream of each MCP gene were amplified by PCR using the primers listed in Table S1. The resulting PCR fragments were fused by either overlap extension PCR (63) or blunt-end ligation. Each product was further amplified by PCR, resulting in a 2-kb fragment with an in-frame deletion of the MCP gene. Each 2-kb DNA fragment was digested with the appropriate restriction enzyme(s) and then inserted into the SpeI site (or the SpeI and SacI sites) of pAW19. The resulting plasmids (Table 4) were used to transform *E. coli* DH5α λ*pir* and introduced into *P. putida* F1 by conjugation in the presence of *E. coli* HB101(pRK2013) as previously described (64). Kanamycin-resistant F1 exconjugants were selected and grown in MSB containing 10 mM succinate. To select for deletion mutants that arose from double-crossover events, cultures were grown in MSB containing 10 mM succinate and 20% sucrose. Individual colonies were then screened for kanamycin sensitivity to confirm the loss of the plasmid, and deletions were verified by PCR using external primers. ΔMCPΔ*aer-2* double mutants were generated by deleting the *aer-2* gene from each MCP single-deletion mutant using the *aer-2* deletion construct pXLF019 (65). The *P. putida* mutant lacking 11 MCP genes (RPF018) was made in the same way by sequential deletion of each MCP gene using the same deletion plasmids as the ones used to generate the single mutants (Table 3), starting with strain XLF017 and sequentially generating GC014, GC105, RPF10, RPF11, RPF14, RPF15, RPF16, RPF17, and RPF18 (F1Δ11). To complement the MCP deletion mutants, relevant MCP genes were PCR amplified using primers listed in Table S1, cut with appropriate restriction enzymes, and cloned into pRK415 (66) or pRK415Km (65). Inserts were verified by restriction digestion and sequencing. Each resulting plasmid was introduced into the single mutant or the F1Δ11 MCP mutant strain (RPF018) by conjugation in the presence of *E. coli* HB101(pRK2013).

***β*-Galactosidase assays.** β-Galactosidase activity was measured at room temperature (approximately 21°C) in chloroform-sodium dodecyl sulfate-permeabilized cells as previously described, and activity is expressed in arbitrary (Miller) units (67). Each culture was assayed in duplicate, and the reported values are the averages from at least three independent experiments.

Method for estimating binding affinity. To estimate the binding affinities of the PcaY-NarQ and NahY-NarQ hybrids, β-galactosidase activity was transformed to relative activity by calculating the difference between the activities of unstimulated cells (no ligand) and stimulated cells (grown in the presence of a specific concentration of the ligand). This transformation allowed relative activity to be plotted against the ligand concentration to generate a nonlinear regression. Using Prism (version 6.0h) software, these data were fit to a Michaelis-Menten kinetic model, $Y = V_{max} \times [L]/(K + [L])$. For this model, Y is the relative activity, V_{max} represents the maximum effect of the ligand, $[L]$ is the concentration of the ligand, and K is the estimated binding affinity.

Quantitative capillary assays. Quantitative capillary assays were carried out as described previously by Liu et al. (68). Briefly, *P. putida* F1 was grown in MSB (59) containing 5 mM 4-hydroxybenzoate (4-HBA) to an OD_{660} of approximately 0.4 and then harvested by centrifugation and resuspended in chemotaxis buffer (CB) (50 mM potassium phosphate buffer [pH 7.0], 0.05% glycerol, 10 μM EDTA) to a final OD_{660} of approximately 0.15. Attractants were tested at concentrations of 0.01, 0.1, 1.0, and 10 mM. Responses to 0.2% Casamino Acids and CB were tested as positive and negative controls, respectively.

Quantitative swim plate assays. Quantitative soft-agar swim plate assays were used to monitor chemotactic responses to propionate (22). For these assays, *P. putida* strains were grown overnight in 2 ml of LB medium at 30°C with shaking. The cultures grown overnight were harvested by centrifugation and resuspended in MSB to an OD_{660} of 0.39 to 0.41, and 2 μl of the suspensions was used to inoculate 15-mm petri plates containing MSB soft agar (0.25%) and 1 mM propionate. When appropriate, 50 μg/ml kanamycin or 12.5 μg/ml tetracycline was included in the medium. Plates without antibiotics were incubated at 30°C for 24 to 26 h, and those containing antibiotics were incubated for 32 to 35 h. Colony images were taken using backlighting (69). Colony diameters were measured, and data are presented as the means ± standard deviations from at least three independent experiments with three technical replicates each. All statistical analyses were conducted using JMP Pro version 14.0.

SUPPLEMENTAL MATERIAL

Supplemental material for this article may be found at https://doi.org/10.1128/AEM.01626-19.

SUPPLEMENTAL FILE 1, PDF file, 0.7 MB.

ACKNOWLEDGMENTS

We thank Cameron Summers, Weston Bodily, Jia Yan, Carissa Eaker, Alexandria Igwe, Victoria Le, Madeline Lee, and Jimmy Kim for carrying out some of the LacZ assays and Xianxian Liu and Grischa Chen for constructing *P. putida* mutants and cloning MCP genes. We also thank three anonymous reviewers for constructive and thoughtful comments on the initial submission.

This work was partially funded by grants from the National Science Foundation to R.E.P. and J.L.D. (MCB 1716833), USDA National Institute of Food and Agriculture Hatch/Evans-Allen/McIntire Stennis project 1020219 (to R.E.P.), and a New Funding Initiative grant from the University of California, Davis, Committee on Research.

REFERENCES

1. Laub MT, Goulian M. 2007. Specificity in two-component signal transduction pathways. Annu Rev Genet 41:121–145. https://doi.org/10.1146/annurev.genet.41.042007.170548.
2. Stewart V. 1993. Nitrate regulation of anaerobic respiratory gene expression in *Escherichia coli*. Mol Microbiol 9:425–434. https://doi.org/10.1111/j.1365-2958.1993.tb01704.x.
3. Appleman JA, Chen LL, Stewart V. 2003. Probing conservation of HAMP linker structure and signal transduction mechanism through analysis of hybrid sensor kinases. J Bacteriol 185:4872–4882. https://doi.org/10.1128/jb.185.16.4872-4882.2003.
4. Stewart V. 2003. Nitrate- and nitrite-responsive sensors NarX and NarQ of proteobacteria. Biochem Soc Trans 31:1–10. https://doi.org/10.1042/bst0310001.
5. Williams SB, Stewart V. 1997. Nitrate- and nitrite-sensing protein NarX of *Escherichia coli* K-12: mutational analysis of the amino-terminal tail and first transmembrane segment. J Bacteriol 179:721–729. https://doi.org/10.1128/jb.179.3.721-729.1997.
6. Williams SB, Stewart V. 1999. Functional similarities among two-component sensors and methyl-accepting chemotaxis proteins suggest a role for linker region amphipathic helices in transmembrane signal transduction. Mol Microbiol 33:1093–1102. https://doi.org/10.1046/j.1365-2958.1999.01562.x.
7. Kirby JR. 2009. Chemotaxis-like regulatory systems: unique roles in diverse bacteria. Annu Rev Microbiol 63:45–59. https://doi.org/10.1146/annurev.micro.091208.073221.
8. Wadhams GH, Armitage JP. 2004. Making sense of it all: bacterial chemotaxis. Nat Rev Mol Cell Biol 5:1024–1037. https://doi.org/10.1038/nrm1524.
9. Bi S, Sourjik V. 2018. Stimulus sensing and signal processing in bacterial chemotaxis. Curr Opin Microbiol 45:22–29. https://doi.org/10.1016/j.mib.2018.02.002.
10. Parkinson JS. 2010. Signaling mechanisms of HAMP domains in chemoreceptors and sensor kinases. Annu Rev Microbiol 64:101–122. https://doi.org/10.1146/annurev.micro.112408.134215.
11. Lacal J, García-Fontana C, Muñoz-Martínez F, Ramos J-L, Krell T. 2010. Sensing of environmental signals: classification of chemoreceptors according to the size of their ligand binding regions. Environ Microbiol 12:2873–2884. https://doi.org/10.1111/j.1462-2920.2010.02325.x.
12. Tso W-W, Adler J. 1974. Negative chemotaxis in *Escherichia coli*. J Bacteriol 118:560–576.
13. Hegde M, Englert DL, Schrock S, Cohn WB, Vogt C, Wood TK, Manson MD, Jayaraman A. 2011. Chemotaxis to the quorum-sensing signal AI-2 requires the Tsr chemoreceptor and the periplasmic LsrB AI-2-binding protein. J Bacteriol 193:768–773. https://doi.org/10.1128/JB.01196-10.
14. Ortega Á, Zhulin IB, Krell T. 2017. Sensory repertoire of bacterial chemoreceptors. Microbiol Mol Biol Rev 81:e00033-17. https://doi.org/10.1128/MMBR.00033-17.
15. Parales RE, Luu RA, Hughes JG, Ditty JL. 2015. Bacterial chemotaxis to xenobiotic chemicals and naturally-occurring analogs. Curr Opin Biotechnol 33:318–326. https://doi.org/10.1016/j.copbio.2015.03.017.
16. Martín-Mora D, Fernández M, Velando F, Ortega Á, Gavira JA, Matilla MA, Krell T. 2018. Functional annotation of bacterial signal transduction systems: progress and challenges. Int J Mol Sci 19:E3755. https://doi.org/10.3390/ijms19123755.
17. Krikos A, Conley MP, Boyd A, Berg HC, Simon MI. 1985. Chimeric chemosensory transducers of *Escherichia coli*. Proc Natl Acad Sci U S A 83:1326–1330. https://doi.org/10.1073/pnas.82.5.1326.
18. Yoshida T, Phadtare S, Inouye M. 2007. The design and development of Tar-EnvZ chimeric receptors. Methods Enzymol 423:166–183. https://doi.org/10.1016/S0076-6879(07)23007-1.
19. Ward SM, Delgado A, Gunsalus RP, Manson MD. 2002. A NarX-Tar chimera mediates repellent chemotaxis to nitrate and nitrite. Mol Microbiol 44:709–719. https://doi.org/10.1046/j.1365-2958.2002.02902.x.
20. Xu Q, Black WP, Mauriello EM, Zusman DR, Yang Z. 2007. Chemotaxis mediated by NarX-FrzCD chimeras and nonadapting repellent responses in *Myxococcus xanthus*. Mol Microbiol 66:1370–1381. https://doi.org/10.1111/j.1365-2958.2007.05996.x.
21. Luu RA, Kootstra JD, Nesteryuk V, Brunton C, Parales JV, Ditty JL, Parales RE. 2015. Integration of chemotaxis, transport and catabolism in *Pseudomonas putida* and identification of the aromatic acid chemoreceptor PcaY. Mol Microbiol 96:134–147. https://doi.org/10.1111/mmi.12929.
22. Parales RE, Luu RA, Chen GY, Liu X, Wu V, Lin P, Hughes JG, Nesteryuk V, Parales JV, Ditty JL. 2013. *Pseudomonas putida* F1 has multiple chemoreceptors with overlapping specificity for organic acids. Microbiology 159:1086–1096. https://doi.org/10.1099/mic.0.065698-0.
23. Hughes JG, Zhang X, Parales JV, Ditty JL, Parales RE. 2017. *Pseudomonas putida* F1 uses energy taxis to sense hydroxycinnamic acids. Microbiology 163:1490–1501. https://doi.org/10.1099/mic.0.000533.
24. Fernández M, Matilla MA, Ortega Á, Krell T. 2017. Metabolic value chemoattractants are preferentially recognized at broad ligand range chemoreceptor of *Pseudomonas putida* KT2440. Front Microbiol 8:990. https://doi.org/10.3389/fmicb.2017.00990.
25. García V, Reyes-Darias JA, Martín-Mora D, Morel B, Matilla MA, Krell T. 2015. Identification of a chemoreceptor for C2 and C3 carboxylic acids. Appl Environ Microbiol 81:5449–5457. https://doi.org/10.1128/AEM.01529-15.
26. Grimm AC, Harwood CS. 1999. NahY, a catabolic plasmid-encoded receptor required for chemotaxis of *Pseudomonas putida* to the aromatic hydrocarbon naphthalene. J Bacteriol 181:3310–3316.
27. El-Gebali S, Mistry J, Bateman A, Eddy SR, Luciani A, Potter SC, Qureshi M, Richardson LJ, Salazar GA, Smart A, Sonnhammer ELL, Hirsh L, Paladin L, Piovesan D, Tosatto SCE, Finn RD. 2019. The Pfam protein families database in 2019. Nucleic Acids Res 47:D427–D432. https://doi.org/10.1093/nar/gky995.
28. Marx RB, Aitken MD. 1999. Quantification of chemotaxis to naphthalene by *Pseudomonas putida* G7. Appl Environ Microbiol 65:2847–2852.
29. Alvarez-Ortega C, Harwood CS. 2007. Identification of a malate chemoreceptor in *Pseudomonas aeruginosa* by screening for chemotaxis defects in an energy taxis-deficient mutant. Appl Environ Microbiol 73:7793–7795. https://doi.org/10.1128/AEM.01898-07.
30. Sampedro I, Parales RE, Krell T, Hill JE. 2015. *Pseudomonas* chemotaxis. FEMS Microbiol Rev 39:17–46. https://doi.org/10.1111/1574-6976.12081.
31. McKellar JL, Minnell JJ, Gerth ML. 2015. A high-throughput screen for ligand binding reveals the specificities of three amino acid chemoreceptors from *Pseudomonas syringae* pv. *actinidiae*. Mol Microbiol 96:694–707. https://doi.org/10.1111/mmi.12964.
32. Fernández M, Morel B, Corral-Lugo A, Krell T. 2016. Identification of a chemoreceptor that specifically mediates chemotaxis toward metabolizable purine derivatives. Mol Microbiol 99:34–42. https://doi.org/10.1111/mmi.13215.
33. Fernández M, Ortega Á, Rico-Jiménez M, Martín-Mora D, Daddaoua A, Matilla MA, Krell T. 2018. High-throughput screening to identify chemoreceptor ligands. Methods Mol Biol 1729:291–301. https://doi.org/10.1007/978-1-4939-7577-8_23.
34. Ni B, Huang Z, Fan Z, Jiang CY, Liu SJ. 2013. *Comamonas testosteroni* uses a chemoreceptor for tricarboxylic acid cycle intermediates to trigger chemotactic responses towards aromatic compounds. Mol Microbiol 90:813–823. https://doi.org/10.1111/mmi.12400.
35. Feng X, Baumgartner JW, Hazelbauer GL. 1997. High- and low-abundance chemoreceptors in *Escherichia coli*: differential activities associated with closely related cytoplasmic domains. J Bacteriol 179:6714–6720. https://doi.org/10.1128/jb.179.21.6714-6720.1997.
36. Weerasuriya S, Schneider BM, Manson MD. 1998. Chimeric chemoreceptors in *Escherichia coli*: signaling properties of Tar-Tap and Tap-Tar hybrids. J Bacteriol 180:914–920.
37. Yang Y, Sourjik V. 2012. Opposite responses by different chemoreceptors set a tunable preference point in *Escherichia coli* pH taxis. Mol Microbiol 86:1482–1489. https://doi.org/10.1111/mmi.12070.
38. Reyes-Darias JA, García V, Rico-Jiménez M, Corral-Lugo A, Lesouhaitier O, Juárez-Hernández D, Yang Y, Bi S, Feuilloley M, Muñoz-Rojas J, Sourjik V, Krell T. 2015. Specific gamma-aminobutyrate chemotaxis in pseudomonads with different lifestyle. Mol Microbiol 97:488–501. https://doi.org/10.1111/mmi.13045.
39. Bi S, Pollard AM, Yang Y, Jin F, Sourjik V. 2016. Engineering hybrid chemotaxis receptors in bacteria. ACS Synth Biol 5:989–1001. https://doi.org/10.1021/acssynbio.6b00053.
40. Ni B, Huang Z, Wu YF, Fan Z, Jiang CY, Liu SJ. 2015. A novel chemoreceptor MCP2983 from *Comamonas testosteroni* specifically binds to *cis*-aconitate and triggers chemotaxis towards diverse organic compounds. Appl Microbiol Biotechnol 99:2773–2781. https://doi.org/10.1007/s00253-014-6216-3.
41. Ames P, Hunter S, Parkinson JS. 2016. Evidence for a helix-clutch mech-

anism of transmembrane signaling in a bacterial chemoreceptor. J Mol Biol 428:3776–3788. https://doi.org/10.1016/j.jmb.2016.03.017.
42. Matilla MA, Krell T. 2017. Chemoreceptor-based signal sensing. Curr Opin Biotechnol 45:8–14. https://doi.org/10.1016/j.copbio.2016.11.021.
43. Pineda-Molina E, Reyes-Darias J-A, Lacal J, Ramos JL, García-Ruiz JM, Gavira JA, Krell T. 2012. Evidence for chemoreceptors with bimodular ligand-binding regions harboring two signal-binding sites. Proc Natl Acad Sci U S A 109:18926–18931. https://doi.org/10.1073/pnas.1201400109.
44. Goldberg SD, Derr P, DeGrado WF, Goulian M. 2009. Engineered single- and multi-cell chemotaxis pathways in *E. coli*. Mol Syst Biol 5:283. https://doi.org/10.1038/msb.2009.41.
45. Derr P, Boder E, Goulian M. 2006. Changing the specificity of a bacterial chemoreceptor. J Mol Biol 355:923–932. https://doi.org/10.1016/j.jmb.2005.11.025.
46. Bi S, Yu D, Si G, Luo C, Li T, Ouyang Q, Jakovljevic V, Sourjik V, Tu Y, Lai L. 2013. Discovery of novel chemoeffectors and rational design of *Escherichia coli* chemoreceptor specificity. Proc Natl Acad Sci U S A 110:16814–16819. https://doi.org/10.1073/pnas.1306811110.
47. Salis H, Tamsir A, Voigt C. 2009. Engineering bacterial signals and sensors. Contrib Microbiol 16:194–225. https://doi.org/10.1159/000219381.
48. Kondoh H, Ball CB, Adler J. 1979. Identification of a methyl-accepting chemotaxis protein for the ribose and galactose chemoreceptors of *Escherichia coli*. Proc Natl Acad Sci U S A 76:260–264. https://doi.org/10.1073/pnas.76.1.260.
49. Manson MD, Blank V, Brade G, Higgins CF. 1986. Peptide chemotaxis in *E. coli* involves the Tap signal transducer and the dipeptide permease. Nature 321:253–256. https://doi.org/10.1038/321253a0.
50. Rico-Jiménez M, Reyes-Darias JA, Ortega Á, Díez Peña AI, Morel B, Krell T. 2016. Two different mechanisms mediate chemotaxis to inorganic phosphate in *Pseudomonas aeruginosa*. Sci Rep 6:28967. https://doi.org/10.1038/srep28967.
51. Ditty JL, Williams KM, Keller MM, Chen GY, Liu X, Parales RE. 2013. Integrating grant-funded research into the undergraduate biology curriculum using IMG-ACT. Biochem Mol Biol Educ 41:16–23. https://doi.org/10.1002/bmb.20662.
52. Liu X. 2009. Chemotaxis to pyrimidines and *s*-triazines in *Pseudomonas* and *Escherichia coli*. PhD dissertation. University of California, Davis, Davis, CA.
53. Corral-Lugo A, De la Torre J, Matilla MA, Fernández M, Morel B, Espinosa-Urgel M, Krell T. 2016. Assessment of the contribution of chemoreceptor-based signalling to biofilm formation. Environ Microbiol 18:3355–3372. https://doi.org/10.1111/1462-2920.13170.
54. Herrera Seitz MK, Soto D, Studdert CA. 2012. A chemoreceptor from *Pseudomonas putida* forms active signalling complexes in *Escherichia coli*. Microbiology 158:2283–2292. https://doi.org/10.1099/mic.0.059899-0.
55. Liu JD, Parkinson JS. 1989. Genetics and sequence analysis of the *pcnB* locus, an *Escherichia coli* gene involved in plasmid copy number control. J Bacteriol 171:1254–1261. https://doi.org/10.1128/jb.171.3.1254-1261.1989.
56. Sambrook J, Fritch EF, Maniatis T. 1989. Molecular cloning: a laboratory manual, 2nd ed. Cold Spring Harbor Laboratory Press, Cold Spring Harbor, NY.
57. Stewart V, Parales J. 1988. Identification and expression of genes *narL* and *narX* of the *nar* (nitrate reductase) locus in *Escherichia coli* K-12. J Bacteriol 170:1589–1597. https://doi.org/10.1128/jb.170.4.1589-1597.1988.
58. Stewart V, Bledsoe PJ. 2003. Synthetic *lac* operator substitutions for studying the nitrate- and nitrite-responsive NarX-NarL and NarQ-NarP two-component regulatory systems of *Escherichia coli* K-12. J Bacteriol 185:2104–2111. https://doi.org/10.1128/jb.185.7.2104-2111.2003.
59. Stanier RY, Palleroni NJ, Doudoroff M. 1966. The aerobic pseudomonads: a taxonomic study. J Gen Microbiol 43:159–271. https://doi.org/10.1099/00221287-43-2-159.
60. Bradford MM. 1976. A rapid and sensitive method for the quantitation of microgram quantities of protein utilizing the principle of protein-dye binding. Anal Biochem 72:248–254. https://doi.org/10.1006/abio.1976.9999.
61. Maniatis T, Sambrook J, Fritsch EF. 1982. Molecular cloning: a laboratory manual. Cold Spring Harbor Laboratory, Cold Spring Harbor, NY.
62. White AK, Metcalf WW. 2004. The *htx* and *ptx* operons of *Pseudomonas stutzeri* WM88 are new members of the Pho regulon. J Bacteriol 186:5876–5882. https://doi.org/10.1128/JB.186.17.5876-5882.2004.
63. Horton RM, Ho SN, Pullen JK, Hunt HD, Cai Z, Pease LR. 1993. Gene splicing by overlap extension. Methods Enzymol 217:270–279. https://doi.org/10.1016/0076-6879(93)17067-f.
64. Simon R, Priefer U, Pühler A. 1983. A broad host range mobilization system for *in vivo* genetic engineering: transposon mutagenesis in gram negative bacteria. Biotechnology (N Y) 1:784–789. https://doi.org/10.1038/nbt1183-784.
65. Luu RA, Schneider BJ, Ho CC, Nesteryuk V, Ngwesse SE, Liu X, Parales JV, Ditty JL, Parales RE. 2013. Taxis of *Pseudomonas putida* F1 toward phenylacetic acid is mediated by the energy taxis receptor Aer2. Appl Environ Microbiol 79:2416–2423. https://doi.org/10.1128/AEM.03895-12.
66. Keen NT, Tamaki S, Kobayashi D, Trollinger D. 1988. Improved broad-host-range plasmids for DNA cloning in Gram-negative bacteria. Gene 70:191–197. https://doi.org/10.1016/0378-1119(88)90117-5.
67. Miller JH. 1972. Experiments in molecular genetics. Cold Spring Harbor Laboratory, Cold Spring Harbor, NY.
68. Liu X, Wood PL, Parales JV, Parales RE. 2009. Chemotaxis to pyrimidines and identification of a cytosine chemoreceptor in *Pseudomonas putida*. J Bacteriol 191:2909–2916. https://doi.org/10.1128/JB.01708-08.
69. Parkinson JS. 2007. A "bucket of light" for viewing bacterial colonies in soft agar. Methods Enzymol 423:432–435. https://doi.org/10.1016/S0076-6879(07)23020-4.
70. Appleman JA, Stewart V. 2003. Mutational analysis of a conserved signal-transducing element: the HAMP linker of the *Escherichia coli* nitrate sensor NarX. J Bacteriol 185:89–97. https://doi.org/10.1128/jb.185.1.89-97.2003.
71. Parales RE, Nesteryuk V, Hughes JG, Luu RA, Ditty JL. 2014. Cytosine chemoreceptor McpC in *Pseudomonas putida* F1 also detects nicotinic acid. Microbiology 160:2661–2669. https://doi.org/10.1099/mic.0.081968-0.
72. Studier FW, Rosenberg AH, Dunn JJ, Dubendorff JW. 1990. Use of T7 RNA polymerase to direct expression of cloned genes. Methods Enzymol 185:60–89. https://doi.org/10.1016/0076-6879(90)85008-c.
73. Finette BA, Subramanian V, Gibson DT. 1984. Isolation and characterization of *Pseudomonas putida* PpF1 mutants defective in the toluene dioxygenase enzyme system. J Bacteriol 160:1003–1009.
74. Gibson DT, Hensley M, Yoshioka H, Mabry TJ. 1970. Formation of (+)-*cis*-2,3-dihydroxy-1-methylcyclohexa-4,6-diene from toluene by *Pseudomonas putida*. Biochemistry 9:1626–1630. https://doi.org/10.1021/bi00809a023.
75. Dunn NW, Gunsalus IC. 1973. Transmissible plasmid coding early enzymes of naphthalene oxidation in *Pseudomonas putida*. J Bacteriol 114:974–979.
76. Figurski DH, Helinski DR. 1979. Replication of an origin-containing derivative of plasmid RK2 dependent on a plasmid function provided in *trans*. Proc Natl Acad Sci U S A 76:1648–1652. https://doi.org/10.1073/pnas.76.4.1648.
77. Zhang X, Hughes JG, Subuyuj GA, Ditty JL, Parales RE. 2019. Chemotaxis of *Pseudomonas putida* F1 to alcohols is mediated by the carboxylic acid receptor McfP. Appl Environ Microbiol 85:e01625-19. https://doi.org/10.1128/AEM.01625-19.